Structural and Functional Characterization of the Human Mdm2 and MdmX RING domains

Olga Egorova

A THESIS SUBMITTED TO THE FACULTY OF GRADUATE STUDIES

IN PARTIAL FULFILLMENT OF THE REQUIREMENTS

FOR THE DEGREE OF

MASTER OF SCIENCE

GRADUATE PROGRAM IN BIOLOGY

YORK UNIVERSITY

TORONTO, ONTARIO

[January 2014]

ABSTRACT

Human E3 ligase Mdm2 is an oncogene. Its amplification and overexpression have been found in many types of cancers. Mdm2 inhibits tumour suppressor p53 by regulating its stability through Mdm2 RING-mediated ubiquitination. Suppression of this process is the promising anti-cancer therapeutic approach. The objectives of this project were to employ biochemical methods to investigate the active site of Mdm2 RING *in vitro* through a mutational analysis of the homologous MdmX RING domain, and to elucidate functions of Mdm2 and MdmX RING *in vivo*. As a result, amino acid residues within the dimerization and E2 binding regions potentially involved in the Mdm2 RING-mediated ubiquitin transfer mechanism were identified. Furthermore, a suppressive effect of the Mdm2 and MdmX RING domains on p53 transcriptional activity was determined *in vivo*. Together, this study provides new insight into the function of Mdm2 RING and opens further perspective on the rational drug design to treat cancer.

ACKNOWLEDGEMENTS

I would like to express my profound and sincere gratitude to my supervisor Dr. Yi Sheng for all her help during my research work documented in this thesis. It was a true privilege to be a part of her group during my undergraduate and graduate studies. I feel very thankful to her for her constant support, patience, trust, and outstanding guidance. I greatly value her suggestions and inspiring ideas throughout my study. I appreciate her criticism and encouragement that not only made this study successful but also developed a better and stronger personality in me. Also, I would like to express my tremendous gratitude for revising my written work.

I would like to thank my advisor Dr. Terrance Kubiseski for his suggestions and advice throughout my graduate study. I would also like to thank Dr. Terrance Kubiseski, Dr. Vivian Saridakis, and Dr. Gerald Audette for being a part of my Master's thesis committee, reviewing, and evaluating my work.

I express my gratitude to Dr. Vivian Saridakis, Dr. Gillian Wu, and Dr. Samuel Benchimol and their groups for support, ideas, and an opportunity to share laboratory equipment and materials.

I would like to thank present and former labmates and friends Rahima Khatun, Anna Troshchynsky, Beena Rishikanth, Raghav Ram, Linda Hu, Veroni Sri, Hossein Davarinejad, Lili Csaniy, Anjali Lobo, Samira Taeb, Jonathan Shloush, Heyam Hayder,

John Vlassov, Philip Tran, Wonsuk Joo, Sachi Kasturia, Woojin Park, and Subin Cho for their support and advice throughout my research experience. I would like to address my special thanks to the undergraduate students who worked with me on this project Heather Lau, Kate McGraphery, and Monika Mis.

I am thankful to Adrienne Dome, Biology Graduate Assistant, for providing help and guidance in completion of the administrative part of the graduate program.

I would not be able to put in words all my gratitude to my sister and my parents for their infinite love, support, encouragement, and sacrifice made for the sake of my future.

Finally, I would like to express my gratitude and appreciation to the Leukemia and Lymphoma Society of Canada, the Banting Research Foundation, and York University for providing financial support in completion of this research work.

ABBREVIATIONS

^{0}C	Degree Celsius
A	Alanine
ATP	Adenosine Tri-Phosphate
C	Cysteine
CFP	Cyan fluorescent protein
Co-IP	Co-Immunoprecipitation
C-terminus	Carboxy-terminus
DNA	Deoxyribonucleic acid
DTT	Dithiothreitol
E	Glutamate
E1	Ubiquitin-activating enzyme
E2	Ubiquitin-conjugating enzyme
E3	Ubiquitin-ligase
FBS	Fetal bovine serum
FL	Full-length
GAPDH	Glyceraldehyde 3-phosphate dehydrogenase
GST-tag	Glutathione S-transferase tag
H	Histidine
His-tag	Hexa-histidine tag
HRP	Horseradish peroxidase
IgG	Immunoglobulin G
IPTG	Isopropyl β-D-1-thiogalactopyranoside

K	Lysine
kDa	Kilodalton
L	Leucine
ml	Millilitre
mM	Millimolar
Mdm2	Mouse double munite 2
MdmX	Mouse double minute X
$MgCl_2$	Magnesium chloride
mRNA	messenger-RNA
N	Asparagine
NaCl	Sodium chloride
N-terminus	Amino-terminus
P	Proline
PBS	Phosphate buffer saline
PCR	Polymerase chain reaction
PMSF	Phenylmethylsulfonyl fluoride
PVDF	Polyvinylidene fluoride
Q	Glutamine
R	Arginine
RING	Really interesting new gene
RNA	Ribonucleic acid
S	Serine
SDS-PAGE	Sodium dodecyl sulpahte - Polyacrylamide gel electrophoresis

T	Threonine
ug	Microgram
uM	Micromolar
V	Valine
YFP	Yellow fluorescent protein

TABLE OF CONTENTS

LIST OF FIGURES

CHAPTER 1: Introduction

1.1. Tumour suppressor p53 as the "Guardian of the Genome"

p53 is a transcription factor, which modulates expression of its target genes to inhibit cell proliferation and promote cell death in response to external stress stimuli, such as DNA-damage, radiation, telomere shortening, oncogene activation, or hypoxia (Gu and Zhu, 2012; Loughery and Meek, 2013). It plays an important role in maintaining genomic integrity and preventing tumourigenesis, thus is known as the "guardian of the genome" (Lane, 1992; Levine, 1997;). p53 was discovered as a binding partner of the viral protein large T antigen in Simian virus 40 (SV40) transformed mouse cell line in 1979 (Chang et al., 1979; DeLeo et al., 1979; Lane and Crawford, 1979; Linzer and Levine, 1979; Melero et al., 1979). Since then, the function of p53 has been extensively studied and shown to be involved in many fundamental cellular processes, including apoptosis, cell cycle, DNA repair, metabolism, senescence, and cell differentiation (Loughery and Meek, 2013). Inactivation of p53 is strongly associated with development of cancer. Indeed, loss of p53 function was found in more than half of all human malignancies caused either by mutation or deletion of the *TP53* gene or aberrant expression of its negative regulators (Vogelstein et al., 2000). Moreover, germline mutations within the *TP53* gene cause Li-Fraumeni syndrome, a rare genetic disease that predisposes affected individuals to development of many types of tumours at a young age (Malkin et al., 1990).

In absence of stress p53 is a short-lived protein and maintained at a low level in cells. Stress signals cause p53 stabilization, activation, and translocation into the nucleus where it regulates transcription of its target genes (Perry, 2010). As a tumour suppressor, p53 primarily targets genes involved in the regulation of apoptosis and cell cycle arrest. p53 induces the expression of pro-apoptotic Bcl-2 family genes, such as *Bax*, *PUMA*, and *Noxa* (Haupt et al., 2003). Upregulation of these genes leads to the release of cytochrome c from mitochondria and induction of apoptosis through activation of caspases (Haupt et al., 2003). p53 also activates the genes involved in cell cycle regulation. Cell cycle arrest is one of the mechanisms of prevention of malignant transformation, which allows damaged cells to have sufficient time to repair damaged DNA. One such p53 target gene is *CDKN1A*, which encodes cyclin-dependent kinase inhibitor 1, known as p21/WAF1. The expression of p21 restrains cell cycle progression from G1 to S phase (el-Deiry et al., 1994). The mechanisms governing how p53 chooses between induction of programmed cell death and inhibition of cell division under stress conditions remain poorly understood; however, it might be dependent on the type of stress and its severity.

p53 consists of 393 amino acid residues with a molecular weight of 53,000 Da (Tang et al., 2008). It possesses an N-terminal transactivation domain (TAD), a proline-rich domain (PRD), a central DNA-binding domain (DBD), a tetramerization domain (TET), and a C-terminal regulatory domain (CTD) (Tang et al., 2008) (Figure 1). In addition, a nuclear localization signal (NLS) and a nuclear export sequence (NES) located at the C-terminus allow p53 to transport in and out of the nucleus (Tang et al., 2008).

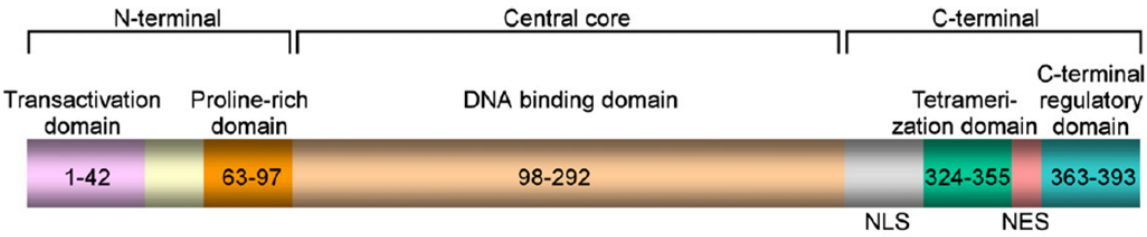

Figure 1. Domain arrangement of p53. Three major functional domains make up p53. N-terminal domain consists of a transactivation domain important for gene transcription activity and a proline-rich domain assisting p53 in its apoptotic activity. Central domain is a DNA binding domain essential for p53 gene transcription activity. C-terminal domain consists of a nuclear localization signal (NLS) and a nuclear export signal (NES) crucial for transport between the nucleus and the cytoplasm. Tetramerization domain is required for gene transcription activity. Regulatory domain is an essential site for post-translational modifications modulating p53 functions. Numbers indicate amino acid residue positions (Adapted from Tang et al., 2008).

TAD and PRD domains are required for the p53-mediated transcriptional regulation. They contain the interaction sites for many transcriptional co-activators and undergo post-translational modifications in response to stresses (Tang et al., 2008). TAD domain was previously shown to interact with TATA-binding protein and play a role in transcription initiation (Chang et al., 1995). PRD was demonstrated to participate in pro-apoptotic and anti-proliferative signaling (Venot et al., 1998; Walker and Levine, 1996). DBD is the main functional domain of p53 and responsible for the interactions with specific p53 target gene promoters (Foord et al., 1991). More than 80% of *TP53* mutations were identified in DBD, implying functional importance of this domain (Rivlin et al., 2011). The active p53 protein forms a tetramer, *i.e.* the complex of four p53 subunits via its TET domain, allowing it to recognize and bind two palindromic DNA sequences (Friedman et al., 1993). In addition, such a complex formation masks NES;

thereby, inhibiting export of p53 out of the nucleus and allowing regulation of gene transcription (Stommel et al., 1999). Finally, CTD is subjected to a variety of post-translational modifications such as phosphorylation, acetylation, methylation, ubiquitination, which modulate p53 function (Tang et al., 2008). Together, these unique structural features enable p53 to quickly integrate stress signals and initiate corresponding cellular responses.

1.2. Post-translational modifications of p53: Role in p53 regulation and function

Post-translational modifications (PTMs) play a crucial role in regulation of p53 activity and function. Almost each p53 domain can be subjected to PTMs; however, majority of the PTMs occur within TAD and CTD domains. Multiple residues of p53 can be phosphorylated, acetylated, methylated, ubiquitinated, sumoylated, neddylated, glycosylated, or ADP-ribosylated (Gu and Zhu, 2012). The interplay among these PTMs determines p53 function.

Under stress conditions cellular p53 is stabilized and activated. Phosphorylation of the N- and C-termini of p53 and acetylation of the C-terminus has been shown to promote p53 stabilization and activation in response to stress signals (Gu and Zhu, 2012; Tang et al., 2008). In particular, serine 15 phosphorylation facilitated stabilization of p53 through inhibiting interaction with its main negative regulator Mdm2, which normally targets p53 for degradation (Dumaz and Meek, 1999). Phosphorylation and acetylation of the C-terminal domain was shown to be critical for activation of gene transcription

activity through induction of the conformational changes exposing p53 DBD and allowing it to interact with DNA (Gu and Roeder, 1997). Other PTMs, such as ubiquitination, sumoylation, and neddylation, are involved in activation or suppression of p53 gene transcription activity through modulating its cellular localization or stability (Gu and Zhu, 2012).

1.2.1. Regulation of p53 through ubiquitination

As p53 activation often leads to growth inhibition and cell death, it is important for the cell to restrain p53 activity in absence of stress signals. p53 ubiquitination is the key mechanism that regulates p53 turnover and keeps p53 levels in check. In this section, the proteins involved in the p53 ubiquitination pathway and their biological functions are discussed.

Ubiquitin is a 76 amino acid regulatory protein found in all eukaryotic cells (Figure 2). It is involved in many cellular functions though a processed called ubiquitination in which ubiquitin molecules are attached to a substrate protein through covalent linkages (Kimura and Tanaka, 2010). It is known that ubiquitination is associated with regulation of protein degradation, cell proliferation, cell growth, development, apoptosis, DNA repair, and signal transduction (Hershko and Ciechanover, 1998). Malfunction of this system can lead to a great number of pathologies, such as development of neurodegenerative disorders, tumours, and defects in the generation of immune responses (Kessler, 2013)

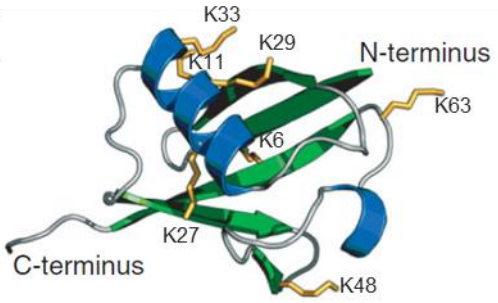

Figure 2. Molecular structure of ubiquitin. Cartoon model of ubiquitin is demonstrated. Seven lysine residues are shown in sticks (Adapted from Brooks, 2010).

p53 ubiquitination involves a series of enzymatic reactions performed by a ubiquitin-activating enzyme E1, a ubiquitin-conjugating enzyme E2, and a ubiquitin ligase E3 (Allende-Vega and Saville, 2010) (Figure 3). E1 enzyme activates ubiquitin in an ATP-dependent manner with formation of a thioester bond between a catalytic cysteine residue of E1 and a C-terminal glycine residue of ubiquitin (Groettrup et al., 2008). Then, ubiquitin is transferred from E1 onto E2 linking ubiquitin to a catalytic cysteine of E2 through a thioester bond (Ye and Rape, 2009). Lastly, E3 enzymes catalyze the transfer of ubiquitin from E2 onto p53 with formation of an isopeptide bond between a C-terminal carboxyl group of ubiquitin and an ε-amino group of lysine of p53 (Dikic et al., 2009; Hammond-Martel et al., 2012; Metzger et al., 2012). There are two E1 enzymes, about 40 E2 enzymes and more than 600 E3 enzymes encoded in a human genome (Allende-Vega and Saville, 2010; Metzger et al., 2012; Ye and Rape, 2009). E3 ligases differ in the way they facilitate ubiquitin transfer and can be classified into E3 HECT enzymes, E3 RING enzymes, and E3 RING-like enzymes (Metzger et al., 2012). The structural and functional diversity of the E3 enzymes provides a great level of specificity for modulating cellular responses.

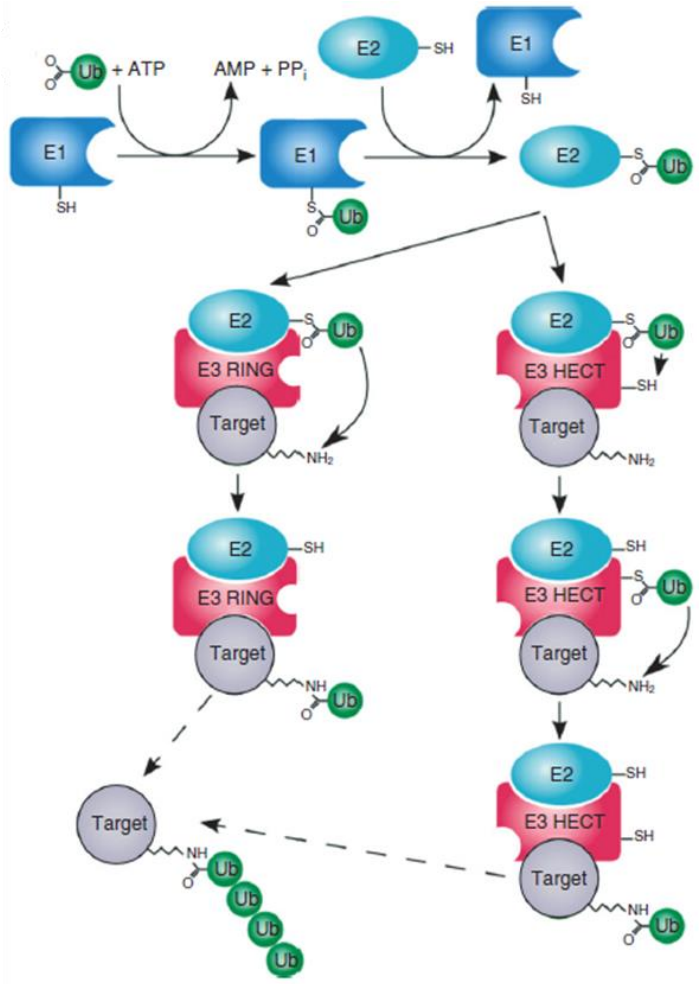

Figure 3. Protein ubiquitination pathway. Protein ubiquitination takes place in several steps. First, ubiquitin is activated in an ATP-dependent manner with a ubiquitin-activating E1 enzyme. Then ubiquitin is transferred onto a ubiquitin-conjugating enzyme E2. The last step is performed by E3 ligases. E3 RING ligases carry out a direct transfer of a ubiquitin molecule from an E2 enzyme onto a substrate protein, while E3 HECT ligases first transfer ubiquitin onto a HECT domain and then onto a target protein (Adapted from Brooks, 2010).

The E3 ligases that have been reported to mediate ubiquitination of p53 include Mdm2, Pirh2, COP1, and ARF-BP1, and depending on the type of ubiquitination pattern, they modulate p53 function differently (Meek and Anderson, 2009). For instance, monoubiquitination results in nuclear export of p53 into the cytoplasm, thus altering its

cellular localization (Marchenko et al., 2007). Mdm2-mediated polyubiquitination of p53 with the formation of lysine 48 ubiquitin chain targets it for degradation by the 26S proteasome (Honda et al., 1997; Thrower et al., 2000). It is the main mechanism that keeps p53 at a low level in unstressed conditions making Mdm2 the main negative regulator of p53 (Honda et al., 1997).

Among these p53 E3 ligases, Mdm2 is the primary E3 ligase and plays a central role in the regulation of p53 function. As the function of Mdm2 is closely linked to its homologous MdmX, the biology of Mdm2 and MdmX and their role in p53 ubiquitination will be discussed below.

1.3. E3 RING ligases Mdm2 and MdmX

1.3.1. Mdm2 and MdmX as the main negative regulators of p53

The human E3 ligase Mdm2, or Murine Double Minute 2, is the main negative regulator of the tumour suppressor p53. The gene encoding for the human E3 ligase Mdm2 was originally identified as an aberrantly amplified DNA fragment on double minute chromosomes in a mouse fibroblast cell line (Fakharzadeh et al., 1993). The importance of Mdm2 for p53 functioning was shown with gene knock-out experiments in mice. Deletion of the *MDM2* gene resulted in lethality in early embryogenesis, where uncontrolled p53 activity caused apoptosis and arrested embryonic development. This phenotype was rescued by knocking out both *TP53* and *MDM2* genes (Jones et al., 1995; Montes de Oca Luna et al., 1995). Mdm2 inhibits the tumour suppressor p53 using two major mechanisms. 1) Mdm2 interacts with the N-terminal transactivation domain of p53

and the interaction abolishes p53 gene transcription activity; 2) Mdm2 mediates both mono- and poly-ubiquitination of p53 (Chen et al., 1995; Momand et al., 1992). Mono-ubiquitination of p53 results in p53 export from the nucleus, whereas polyubiquitination targets p53 for the proteasomal degradation (Geyer et al., 2000; Gu et al., 2001; Haupt et al., 1997; Honda et al., 1997; Kubbutat et al., 1997). p53 and Mdm2 form an autoregulatory negative feedback loop to keep p53 level under control (Wu et al., 1993). *MDM2* is a p53 target gene; therefore, activation of p53 under stress conditions induces expression of Mdm2. The increased levels of Mdm2 act to suppress p53 activity and switch off the p53 responses (Wu et al., 1993).

Murine Double Minute X (MdmX, also known as Mdm4) is another important negative regulator of p53. MdmX is homologous to Mdm2 in arrangement of domains and function (Shvarts et al., 1996; Shvarts et al., 1997). Its relationship to p53 function was demonstrated through gene knockout experiments. *MDMX* gene knockout resulted in embryonic lethality in the early developmental stage due to excessive p53 activity; however, knocking out both *MDMX* and p53 rescued embryonic lethality (Parant et al., 2001). This experiment not only showed the importance of MdmX for p53 regulation, but also showed the requirement for presence of both Mdm2 and MdmX for proper p53 functioning. N-terminal p53-binding domain of MdmX interacts with the N-terminal transactivation domain of p53 and inhibits its gene transcription activity (Bottger et al., 1999). MdmX lacks intrinsic E3 ligase activity; however, it dimerizes with Mdm2 and regulates p53 ubiquitination in an indirect way (Sharp et al., 1999; Stad et al., 2001; Tanimura et al., 1999).

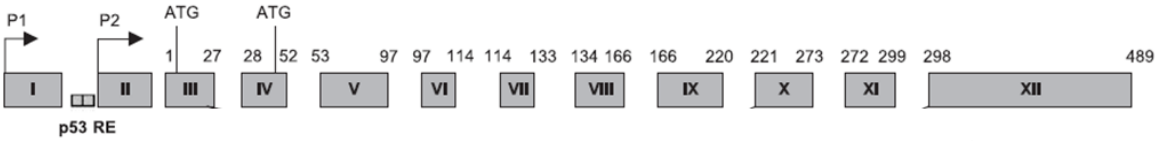

Figure 4. Structure of the *MDM2* gene. The gene consists of 12 exons and two p53 responsive elements (indicated as p53 RE). The gene possesses two promoters P1 and P2 and two start codons in exons 3 and 4. Numbers indicate amino acid residue positions, and roman numbers indicate exons (Adapted from Iwakuma and Lozano, 2003).

1.3.2. Gene structure and protein domains

The *MDM2* gene is located on chromosome 12. It consists of 12 exons and two promoters, the second of which is p53-dependent (Iwakuma and Lozano, 2003) (Figure 4). The *MDMX* gene is located on chromosome 1 and includes 11 exons, and the *MDMX* gene is not under p53 transcriptional regulation (Lenos and Jochemsen, 2011) (Figure 5). Figure 6 depicts domain organization of Mdm2 and MdmX. Both Mdm2 and MdmX proteins contain N-terminal p53-binding domains that interact with the p53 transactivation domain and negatively regulate p53 transcription activity (Bottger et al., 1999; Chen et al., 1995; Momand et al., 1992; Oliner et al, 1992).

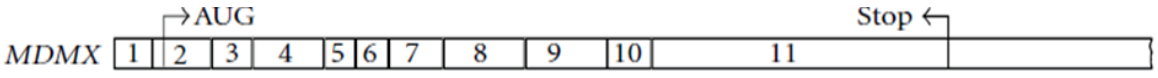

Figure 5. Structure of the *MDMX* gene. The gene consists of 11 exons, one start codon in exon 2. Stop codon is indicated in exon 11 (Adapted from Lenos and Jochemsen, 2011).

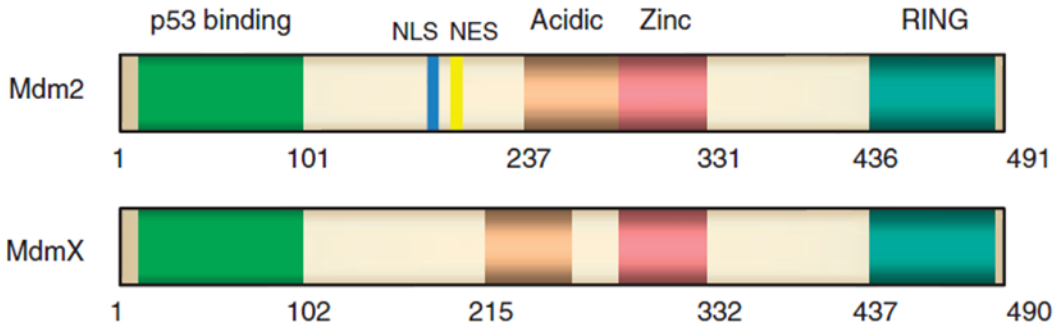

Figure 6. Protein domain arrangement of Mdm2 and MdmX. Both Mdm2 and MdmX possess N-terminal p53-binding domains (green), central acidic domains (orange), zinc finger domains (red), and C-terminal RING domains (cyan). Mdm2 alone contains a nuclear localization signal (NLS, blue) and a nuclear export sequence (NES, yellow). Numbers indicate amino acid residue positions (Adapted from Lee and Gu, 2010).

Mdm2 possesses a nuclear localization signal and a nuclear export sequence facilitating Mdm2 translocation between the nucleus and the cytoplasm, which enables Mdm2 to tightly regulate p53 function (Roth et al., 1998; Tao and Levine, 1999). In contrast, MdmX lacks those signals and is primarily localized in the cytoplasm when it is ectopically overexpressed in a cell (Li et al., 2002). However, most endogenous MdmX is observed within the nucleus as it dimerizes with Mdm2, and dimerization promotes its translocation into the nucleus (Li et al., 2002). Furthermore, Mdm2 contains a central acidic domain and a zinc finger domain, both of which participate in p53 ubiquitination (Kawai et al., 2003; Lindstrom et al., 2007). MdmX also possesses an acidic domain and a zinc finger domain. However, there is little sequence similarity between MdmX and Mdm2 within these two domains, and the role of the MdmX acidic domain and zinc finger domain is not clear. In addition, Mdm2 possesses a nucleolar localization signal within the C-terminal domain helping retain Mdm2 within the nucleolus during stress

response, a mechanism allowing p53 to regulate gene transcription (Lohrum et al., 2000). Finally, both Mdm2 and MdmX contain C-terminal RING domains. The Mdm2 RING domain is the catalytic site for its E3 ligase activity. Although the MdmX RING domain shares a high degree of sequence homology with the Mdm2 RING domain, it does not contain E3 ligase activity. Both domains are crucial for the function of Mdm2 and MdmX. As Mdm2 and MdmX RING domains are the focus of my study, their structural and functional features are further discussed in the next section.

1.3.3. Mdm2 RING domain: A key to ubiquitin transfer

A RING (Really Interesting New Gene) finger domain is a protein structural motif consisting of approximately 60 amino acids. The main role of the RING domain is to recruit a ubiquitin conjugating enzyme E2 and perform a direct transfer of ubiquitin from an E2 enzyme onto a substrate protein. The RING finger domain is a cysteine and histidine rich zinc binding motif (Freemont et al., 1993). It coordinates two zinc ions by four pairs of cysteine and histidine residues and folds into a cross-braced topology, i.e. the first and third pairs of cysteine and histidine residues coordinate the first zinc ion and the second and fourth pairs of cysteine residues bind to the second zinc ion (Freemont et al., 1993). This is an essential feature the RING domain and is important for its structural stability and its catalytic function.

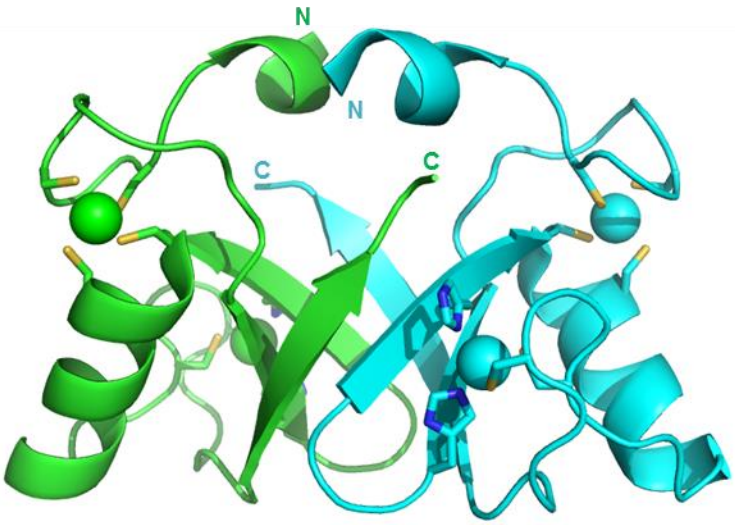

Figure 7. Crystal structure of the Mdm2/MdmX RING heterodimer. Mdm2 RING (432-491) subunit is coloured in green; MdmX RING (430-490) subunit is coloured in cyan (PDB 2VJE). Each RING subunit coordinates two zinc ions with cysteine and histidine residues shown in sticks. Amino- and carboxy-termini are indicated as N and C, respectively. Protein model was generated using PyMol software.

The Mdm2 and MdmX RING domains are located at the extreme C-termini of Mdm2 and MdmX. Figure 7 demonstrates the crystal structure of the Mdm2/MdmX RING heterodimer. Sequence alignment of the Mdm2 and MdmX RING domains shows conservation of the cysteine and histidine residues involved in coordination of two zinc ions (Figure 8A). Removal of zinc ions by using metal-chelating reagents, such as EDTA, or mutations of the cysteine and histidine residues harbouring zinc ions led to inactivation of the Mdm2 RING domain-mediated E3 ligase activity (Fang et al., 2000).

Despite the fact that MdmX RING is structurally homologous to Mdm2 RING, MdmX RING does not have E3 ligase activity. MdmX modulates Mdm2 E3 ligase

activity by inhibiting Mdm2 autoubiquitination and stabilizing Mdm2 through formation of the Mdm2/MdmX heterodimer via RING domains.

Several research studies attempted to define regions of the Mdm2 RING domain required for dimerization and for E2 binding, which are two essential features required for E3 ligase activity. Mutagenesis of the last five C-terminal residues within the Mdm2 RING domain abolished E3 ligase activity and dimerization (Poyurovsky et al., 2007). Similarly, mutational analysis of the seven extreme C-terminal residues of the Mdm2 RING domain diminished Mdm2 E3 ligase activity; however, deletion of those residues attenuated dimerization and ubiquitination activity (Shloush et al., 2010). Mdm2/Mdm2 and Mdm2/MdmX dimerization was further revealed by the solution and crystal structures of the Mdm2/Mdm2 RING homodimer and Mdm2/MdmX RING heterodimer, respectively (Kostic et al., 2006; Linke et al., 2008). Indeed, investigation of the Mdm2/MdmX RING crystal structure revealed contacts between the β3-stand of one subunit and β2-strand of the other subunit, thus forming a β-barrel structure composed of six β-strands. These results suggest that the C-terminal residues are essential for the Mdm2 RING domain-mediated E3 ligase activity. Further mutational analysis identified a number of amino acid residues located within the loop regions and the α-helix required for interactions with an E2 enzyme (Linke et al., 2008; Shloush et al., 2010). Although dimerization region of the RING domain and the E2 binding surfaces have been mapped, the mechanism of the Mdm2 RING-mediated E3 ligase activity particularly how the RING domain mediates ubiquitin transfer from an E2 enzyme onto a substrate remains elusive and requires further investigation.

1.4. Mdm2 and MdmX in human diseases

Many types of human cancers are characterized by gene amplification or overexpression of Mdm2 and MdmX. Mdm2 is overexpressed in 7% of all human cancers and 30% of osteogenic and soft tissue sarcomas (Momand et al., 1998). Amplification of the *MDMX* gene was found in about 35% of osteogenic and 16% of soft tissue sarcomas (Lenos et al., 2012). In addition, aberrant *MDM2* and *MDMX* gene products have been identified. More than 40 alternatively spliced *MDM2* forms have been found in normal and cancerous tissues (Volk et al., 2009). *MDM2* splice variants were detected primarily in malignant tumour types with poor prognosis (Dang et al., 2002). Although mechanisms are not clear, it is believed that alternative splicing of Mdm2 mRNA transcripts, proteolytic cleavage, or post-translational modifications lead to expression of aberrant protein products (Evans et al., 2001; Volk et al., 2009). MDM2-A and $HDM2^{ALT1}$ are the *MDM2* splice variants lacking the N-terminal p53 binding domain, however, containing the intact C-terminal RING domain (Evans et al., 2001; Volk et al., 2009). These splice variants were found to interact with the full-length Mdm2 *in vivo* and interfere with the Mdm2-mediated p53 inactivation (Evans et al., 2001; Volk et al., 2009). Similar to *MDM2* gene, *MDMX* gene was also found to undergo alternative splicing (Giglio et al., 2005). An *MDMX* splice variant, *HDMX211*, lacking the N-terminal p53 binding domain and containing the intact C-terminal RING domain was identified (Giglio et al., 2005). *HDMX211* was found to interact and stabilize Mdm2 and counteract with its ability to target p53 for degradation (Giglio et al., 2005).

1.5. Inhibition of Mdm2 and MdmX

Aberrant amplification of the *MDM2* and *MDMX* genes and overexpression of their gene products are clearly associated with cancer development. Therefore, developing therapeutics to inhibit Mdm2 and MdmX in cancer cells is a desired strategy and needs to be pursued for anticancer therapy. Development of Mdm2 inhibitors follows three main strategies: suppression of Mdm2 expression, disruption of the Mdm2/p53 interaction, and eradication of its E3 ligase activity. Introduction of anti-sense oligonucleotides and siRNA targeting Mdm2 mRNA led to an increase in stabilization and activation of the p53 apoptotic function (Chen et al., 1998; Tortora et al., 2000; Zhang et al., 2003). The second approach is to interfere with the interaction between the N-terminal domain of Mdm2 and the transactivation domain of p53. Small-molecule inhibitors have already been identified and shown to inhibit Mdm2-mediated inactivation of p53 gene transcription activity, such as Nutlins, RITA, MI-63, and MI-219 (Ding et al., 2006; Issaeva et al., 2004; Shangary et al., 2008; Vassilev et al., 2004). The third approach is to inhibit E3 ligase activity of the Mdm2 C-terminal RING domain. High-throughput screening of chemical compounds revealed several classes of inhibitors, such as HLI98, HLI373, and sempervirine, able to suppress Mdm2-mediated autoubiquitination and p53 ubiquitination leading to a stabilized and activated cellular p53 (Kitagaki et al., 2008; Sasiela et al., 2008; Yang et al., 2005). Structural characterization of the binding interface between the N-terminal p53-binding domain of Mdm2 and the N-terminal p53 transactivation domain enables development of inhibitors that dissociate interaction between Mdm2 and p53. However, the catalytic site of the Mdm2 RING domain remains

poorly characterized. This limits development of inhibitors targeting Mdm2 E3 ligase activity. Further characterization of the Mdm2 RING domain will allow improvement of the existing Mdm2 E3 ligase inhibitors and enable development of novel compounds that exhibit potency and selectivity in targeting E3 ligase activity of Mdm2.

1.6. Objectives

Under stress conditions the tumour suppressor p53 prevents malignant transformation by promoting apoptosis or cell cycle arrest. Absence of the normal function of p53 as a tumour suppressor promotes tumourigenesis. In cancer cells p53 activity is inhibited by gene amplification or overexpression of its main negative regulators homologous E3 ligases Mdm2 and MdmX. Therefore, developing inhibitor compounds targeting Mdm2 and MdmX is a desired anti-cancer therapeutic approach. Research has been mostly concentrated on inhibiting Mdm2 and MdmX N-termini to re-activate p53 gene transcription activity. However, it is as important to eliminate Mdm2-mediated p53 ubiquitination by means of inhibiting the Mdm2 RING domain. Current drug design targeting the Mdm2 RING domain lacks effectiveness due to insufficient knowledge in the mechanistic details of the Mdm2 RING-mediated ubiquitination. In this study, I characterize the Mdm2 and MdmX RING domains in order to provide a mechanistic insight into the Mdm2 RING-mediated ubiquitination.

In the *in vitro* study, I aim to identify the amino acid residues important for the Mdm2 RING-mediated ubiquitin transfer mechanism. I hypothesize that the sequence differences between the Mdm2 and MdmX RING domains are responsible for their

functional differences. I performed site-directed mutagenesis of the MdmX RING domain and characterized the role of each mutated residue in the RING domain-mediated ubiquitination. This project was initiated during my fourth year Undergraduate Honours Thesis in Dr. Yi Sheng's lab. As an undergraduate student I established methodology and was able to synthesize several MdmX RING domain mutants and test their autoubiquitination activity *in vitro*. As a graduate student I performed extensive sequence alignment and structural analyses, reproduced my previous findings, and performed additional *in vitro* ubiquitination assays to test activities of the mutated MdmX RING domains.

In the *in vivo* study, I aim to investigate functions of the Mdm2 and MdmX RING domains. I examined effects of the ectopic expression of Mdm2 RING and MdmX RING on the endogenous levels of Mdm2, MdmX, and p53. I also investigated effects on transcriptional activity of p53 by analyzing levels of phosphorylated p53, p21, and Bax. Finally, I characterized cellular localization of the overexpressed Mdm2 RING and MdmX RING and examined interactions of the ectopically expressed Mdm2 RING and MdmX RING with full-length Mdm2 and MdmX.

CHAPTER 2: Structural and functional characterization of the active site of the human Mdm2 RING domain

2.1. Introduction

Mdm2 is strongly associated with cancer development and progression. The *MDM2* gene is found amplified or overexpressed in 7% of all human cancers; therefore, finding ways of inhibiting Mdm2 in cancer cells and restoring p53 function is a rational therapeutic approach (Momand et al., 1998). For instance, a small molecule inhibitor, Nutlin, was developed to block interactions between the N-termini of Mdm2 and p53, thereby, inhibiting p53 transcription activity (Vassilev et al., 2004). However, there is limited progress in development of Mdm2 inhibitors targeting its E3 ligase activity. Ubiquitination activity of Mdm2 is attributed to its C-terminal RING domain, which performs a direct transfer of ubiquitin from an E2 enzyme onto a substrate protein. Several research studies have made attempts to characterize the RING domain-mediated ubiquitin transfer mechanism; however, mechanistic details still remain poorly understood (Iyappan et al., 2010; Linke et al., 2008; Shloush et al., 2011). Lack of understanding of how the RING domain works represents a major drawback in developing Mdm2 E3 ligase inhibitors.

This study provides a further insight into the mechanism of the Mdm2-mediated ubiquitination through analyzing functional differences between the Mdm2 and MdmX RING domains. It is hypothesized that amino acid differences between these two RING domains might be responsible for their functional differences. To test this hypothesis,

sequence and structure analyses of the Mdm2 RING and MdmX RING domains were performed to identify the Mdm2 RING residues that differed between Mdm2 and MdmX and could potentially be responsible for E3 ligase activity. Based on their structural proximity to the active site and evolutionary sequence conservation, several Mdm2 RING residues were chosen and substituted in the MdmX RING domain through site-directed mutagenesis. *In vitro* ubiquitination assays were performed to test whether the mutated MdmX RING domain could gain E3 ligase activity.

2.2. Materials and Methods

2.2.1. *Molecular cloning and site-directed mutagenesis*

MdmX RING (416-491) was cloned from the human MdmX (1-491) into NdeI/BamHI digested pET-15b (Novagene) and pGEX-2TK (GE) expression vectors. Mutagenesis of the MdmX RING domain was carried out using QuikChange® Site-Directed Mutagenesis Kit.

2.2.2. *Protein expression and purification*

All proteins were expressed in *Escherichia coli* BL21 DE3 Codon Plus cells (Stratagene) using 1 mM IPTG for 16 hours at 16 ^{o}C. 150 uM $ZnCl_2$ was added to the growing bacterial cultures. To prepare His-fusion proteins, bacterial pellets were sonicated in lysis buffer (50 mM Tris pH 7.5, 500 mM NaCl, 10% glycerol, 50 uM $ZnCl_2$, 1 mM benzamidine, 0.5 mM PMSF, 1 mM β-mercaptoethanol, 0.1% Triton-X, 20 mM imidazole). Following 1 hour incubation with nickel resin, samples were washed

with a buffer containing 50 mM Tris pH 7.5, 500 mM NaCl, 10% glycerol, 50 uM $ZnCl_2$, 1 mM benzamidine, 0.5 mM PMSF, 1 mM β-mercaptoethanol, and 20 mM imidazole. His-RING domains were eluted from the resin with elution buffer (50 mM Tris pH 7.5, 500 mM NaCl, 10% glycerol, 50 uM $ZnCl_2$, 1 mM benzamidine, 0.5 mM PMSF, 1 mM β-mercaptoethanol, 500 mM imidazole). For purification of the GST-fusion RING domains, cell pellets were sonicated in a buffer containing 50 mM Tris pH 7.5, 500 mM NaCl, 10% glycerol, 50 uM $ZnCl_2$, 0.5 mM PMSF, 10 mM β-mercaptoethanol, and 0.1% Triton-X. Samples were washed with wash buffer (50 mM Tris pH 7.5, 500 mM NaCl, 10% glycerol, 50 uM $ZnCl_2$, 0.5 mM PMSF, 10 mM β-mercaptoethanol) after 2-hour incubation with the GST resin. GST-fusion proteins were eluted in a buffer containing 50 mM Tris, 30 mM glutathione, 500 mM NaCl, 10% glycerol, 50 uM $ZnCl_2$, 10 mM β-mercaptoethanol in pH 7.5. All protein samples were stored at -80 ^{o}C until use.

2.2.3. *In vitro ubiquitination assays*

A ubiquitination reaction contained 0.5 ug of E1, 0.2 ug of UbE2D2, and 5 ug of ubiquitin. For autoubiquitination assays, 0.5 ug of E3 (His-tagged RING domains) was used; for substrate ubiquitination, a total of 1.0 ug of E3 was used (0.5 ug of His-tagged RING domains and 0.5 ug of either GST-MdmX RING domain or GST-MdmX full-length). The reaction was performed in 20 ul of the buffer containing 50 mM Tris pH 7.6, 5 mM MgCl2, 2 mM DTT, 0.1X protease inhibitor, and 2 mM ATP. Following 90-minute incubation at 30 ^{o}C, 5x SDS-PAGE sample buffer was added to reactions which were later resolved on 7.5% SDS-PAGE and transferred onto the PVDF membrane

(GE Healthcare Amersham HybondTM-P) for immunoblotting. Autoubiquitination of the RING domains was detected using a monoclonal anti-ubiquitin antibody (Covance). Substrate ubiquitination was visualized using a monoclonal anti-GST antibody (GE Healthcare).

2.2.4. *Protein modeling*

Protein complex modeling and mutagenesis were performed using PyMol software. Solution structure of the Mdm2 RING homodimer (PDB 2HDP) and crystal structure of the Mdm2/MdmX RING heterodimer (PDB 2VJE) were used to demonstrate wild-type protein complexes (Kostic et al., 2006; Linke et al., 2008). The model of the MdmX RING homodimer was generated using the crystal structure of the Mdm2/MdmX RING heterodimer (PDB 2VJE). The model of the E2-E3 complex was generated using the crystal structure of the cIAP2-UbcH5B complex (PDB 3EB6) and the crystal structure of the Mdm2/MdmX RING heterodimer (PDB 2VJE) (Linke et al., 2008; Mace et al., 2008). The Mdm2 RING and MdmX RING subunits were aligned with the cIAP2 RING domain, and the cIAP2 RING domain was not shown in the figure to facilitate viewing of the complex between the aligned Mdm2 and MdmX RING domains and UbcH5B E2 enzyme.

2.3. Results

2.3.1. Sequence and structural analysis of the Mdm2 and MdmX RING domains

As the sequence and structural variations between the Mdm2 and MdmX RING domains are responsible for the functional differences, a sequence and structural analyses of the Mdm2 and MdmX RING domains were performed to map the catalytic site of the Mdm2 RING domain. Based on the sequence alignment of the Mdm2 and MdmX RING domains from several species, the Mdm2 RING domain is more conserved throughout evolution than the MdmX RING domain; however, the two domains share about 43% sequence identity (Figure 8A). There are 25 highly conserved residues identified, which form the core structure of the RING domain composed of two β-strands and one α-helix. Among these conserved residues, six cysteines and two histidines, are important for coordination of two zinc ions, which were also shown to be essential for proper folding of the RING domain (Fang et al., 2000). There are 36 residues that are different between the Mdm2 and MdmX RING domains and share various degrees of conservation. 27 of those amino acid changes possess side chains with similar chemical properties. For instance, there is isoleucine at position 435 within Mdm2 RING, and there is leucine at the corresponding MdmX RING position. Both residues are hydrophobic. The remaining 9 amino acid differences carry side chains with differing chemical properties. For instance, Mdm2 RING possesses a hydrophobic valine residues at position 439, whereas MdmX RING – a polar serine residue at the same position.

A.

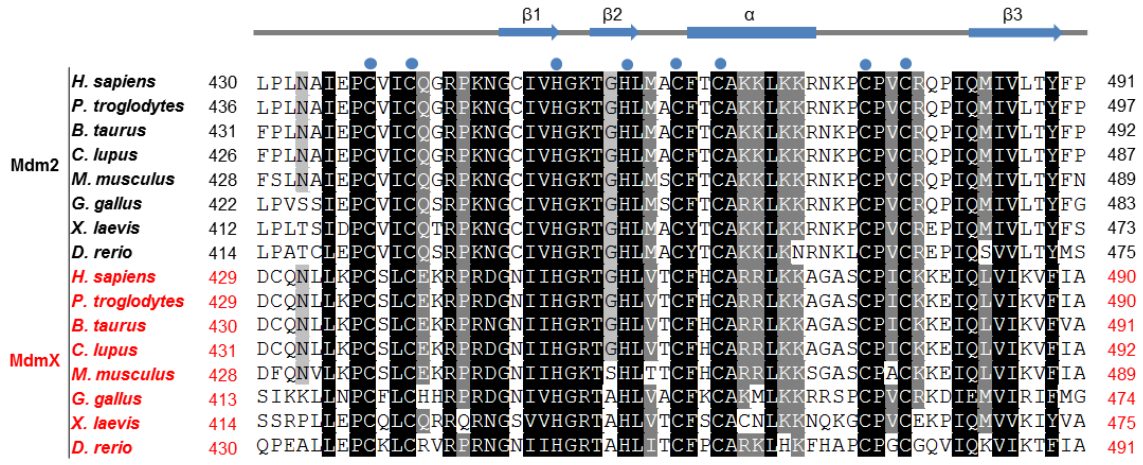

B.

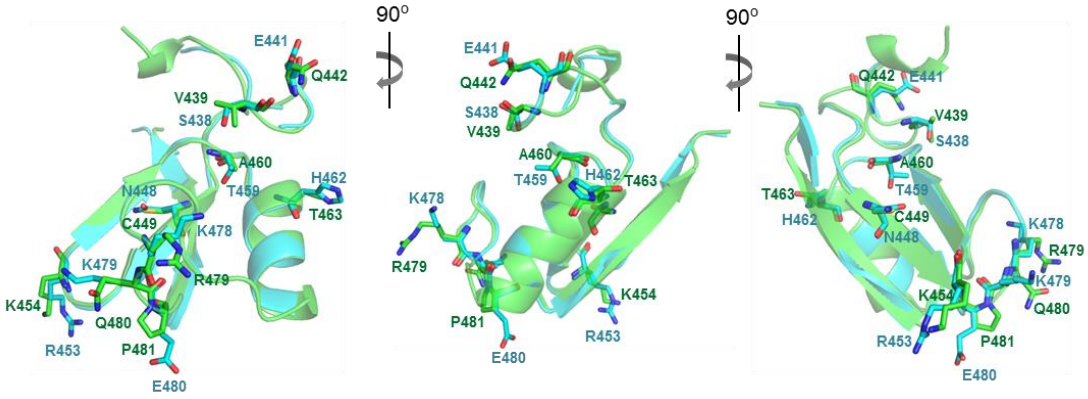

Figure 8. Sequence and structure analysis of the Mdm2 and MdmX RING domains. *A*, Sequence alignment of the Mdm2 and MdmX RING domains from different species is depicted. Residues between the Mdm2 and MdmX RING domains are shaded based on their sequence conservation. The secondary structure of the RING domain is shown on top. The cysteine and histidine residues involved in zinc coordination are indicated by blue circles. The MdmX RING mutated residues are shown with red and blue stars. The protein accession numbers for the Mdm2 RING domains are as follows *H. sapiens* (Q00987.1), *P. troglodytes* (XP_001155208.1), *B. taurus* (NP_001092577.1), *C. lupus* (NP_001003103.1), *M. musculus* (NP_0349116.1), *G. gallus* (NP_001186313.1), *X. laevis* (P56273), *D. rario* (NP_571439.2). The protein accession numbers for the MdmX RING domains are as follows *H. sapiens* (NP_002384.2), *P. troglodytes* (XP_001160152.1), *B. taurus* (NP_001039634.1), *C. lupus* (XP_536098.3), *M. musculus* (NP_032601.2), *G. gallus* (XP_417957.3), *X. laevis* (NP_001082434), *D. rario* (NP_997897.1). The sequence alignment was performed by ClustalX2.1 and presented using GeneDoc. *B*, Model representing the aligned Mdm2 RING and MdmX RING domains (PDB 2VJE) is demonstrated. Mdm2 RING subunit is shown in green, MdmX RING – in cyan. Mdm2 and MdmX RING residues under investigation are shown in sticks.

The crystal structure of the Mdm2/MdmX RING domain heterodimer (PDB 2VJE) was used to analyze the positions of the non-identical amino acids and predict their functional importance. We selected Mdm2 RING cysteine 449 (C449) and lysine 454 (K454) located within the hydrophobic core of the RING domain dimer, as well as valine 439 (V439), glutamine 442 (Q442), alanine 460 (A460), threonine 463 (T463), arginine 479 (R479), glutamine 480 (Q480), and proline 481 (P481) located at the putative E2 enzyme interaction surface (Figure 8B). These residues are located within the loop regions of the RING domain (except for C449 located within β1-strand and T463 located within the α-helix) in close proximity to the zinc coordination sites (Figures 9A and 9B). High degree of conservation of these residues within the Mdm2 RING domain across several species analyzed in this study suggest that they might play a role in maintaining structural integrity of the Mdm2 RING domain or contribute to E3 ligase activity (Figure 8A). Moreover, the fact that these residues were not conserved between Mdm2 and MdmX proposed the possibility of these residues being responsible for E3 ligase activity of the Mdm2 RING domain. To test, this hypothesis, site-directed mutagenesis of the MdmX RING domain was performed.

2.3.2. Mutational analysis of the MdmX RING domain

Using site-directed mutagenesis, selected Mdm2 RING residues were introduced into the MdmX RING domain at the corresponding sites. Specifically, arginine 453 and asparagine 448 within the core of the Mdm2/MdmX RING heterodimer were substituted for lysine and cysteine, respectively and known as R453K and N448C. Moreover, the potential E2 binding surface mutations serine 438 to valine (S438V), glutamate 441 to glutamine (E441Q), threonine 459 to alanine (T459A), histidine 462 to threonine (H462T), lysine 478 to arginine (K478R), lysine 479 to glutamine (K479Q), and glutamate 480 to proline (E480P) were introduced into the MdmX RING domain. Figures 9A and 9B show the localization of the selected residues within the Mdm2 and MdmX RING domains and the summary of the generated MdmX RING domain mutants. In this study, three single MdmX RING domain mutants – N448C, T459A, and K478R, four double mutants – S438V/E441Q, N448C/K478R, R453K/K478R, and T459A/H462T, and one triple mutant – KKE478RQP were generated.

Mutant MdmX RING domains were expressed in *E. coli* as His-tag fusion proteins and purified using nickel affinity chromatography (Appendix B. Figures 3 and 4). They were used to test their E3 ligase activity through *in vitro* ubiquitination assays.

A.

B.

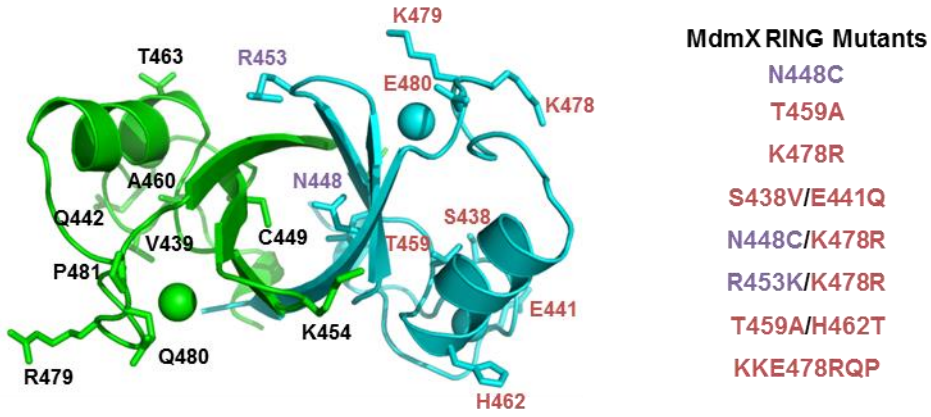

Figure 9. Mutational analysis of the MdmX RING domain. *A,* Sequence alignment of the Mdm2 RING (430-491) and MdmX RING (429-490) is shown. Conserved cysteine and histidine residues involved in zinc ion coordination are highlighted in orange. Mutated residues potentially involved in dimerization are highlighted in purple, and mutated residues potentially involved in E2 binding – in red. *B,* Cartoon model representing Mdm2/MdmX RING heterodimer (PDB 2VJE) is depicted. Mdm2 RING subunit is shown in green, MdmX RING – in cyan. MdmX RING mutated residues are shown in sticks and labeled in purple and red. The corresponding Mdm2 RING residues are shown in sticks and labeled in black. Summary of the generated MdmX RING domain mutants is shown in table on the right.

2.3.3. Autoubiquitination activity of the MdmX RING mutants

MdmX RING domain mutants were first tested for the ability to perform autoubiquitination, that is ubiquitination of the E3 (wild-type and mutated MdmX RING domains) itself, using *in vitro* ubiquitination assay (Figures 10A and 10B). In this assay, wild-type Mdm2 RING was used as the positive control and wild-type MdmX RING as the negative control. Each reaction included E1, E2 (UbE2D2/UbcH5B), His-tagged E3 (Mdm2 RING, MdmX RING, or MdmX RING mutant), His-tagged ubiquitin, and ATP. The efficiency of the E3 ligase in each reaction was evaluated based on the amount of the ubiquitinated substrates produced, which was detected by immunoblotting using an antibody against ubiquitin (Figure 10B). The results of the experiment are summarized in Figure 10C. As expected, Mdm2 RING domain demonstrated strong autoubiquitination activity. MdmX RING T549A and KKE478RQP mutants did not show any autoubiquitination activity. MdmX RING K478R, T459A/H462T, S438V/E441Q, and R453K/K478R mutants gained weak ubiquitination activity. Interestingly, a point mutation N448C and a double mutation N448C/K478R granted MdmX RING domain an ability to ubiquitinate itself similar to Mdm2 RING domain suggesting the respective residues Mdm2 C449 and R479 play important roles in the Mdm2-mediated ubiquitination.

A.

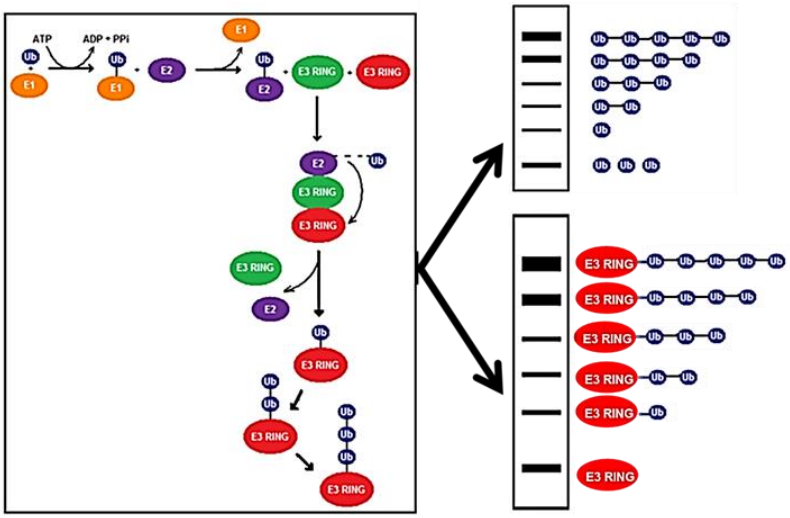

B.

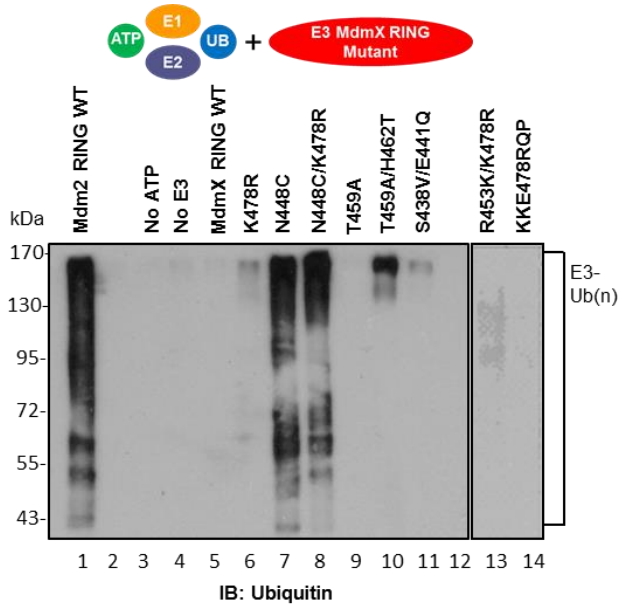

C.

E3 ligase	Activity
Mdm2 RING WT	++++
MdmX RING WT	---
K478R	+
N448C	+++
N448C/K478R	+++
T459A	---
T459A/H462T	++
S438V/E441Q	+
R453K/K478R	+
KKE478RQP	---

Figure 10. Autoubiquitination activity of the MdmX RING mutants. *A,* Principle of the *in vitro* ubiquitination assay. *B,* Autoubiquitination activity of the Mdm RING domains was investigated with *in vitro* ubiquitination assay which included E1, E2 (E2D2), E3 (either His Mdm2 RING in positive and negative controls or His MdmX RING in experimental samples), ubiquitin, and ATP as described in Section 2.2.3. Autoubiquitination activity was detected using a monoclonal anti-ubiquitin antibody (Covance) *C,* E3 ligase activity exhibited by the wild-type Mdm2 and MdmX RING domains, as well as of the mutated MdmX RING domains is estimated based on the strength of the signal and is summarized in the table.

2.3.4. Ubiquitination of the wild-type MdmX RING and the wild-type full-length MdmX by the mutated MdmX RING domains

Following autoubiquitination, the MdmX RING domain mutants were tested for the ability to perform substrate ubiquitination (Figure 10A). As MdmX is one of the ubiquitination substrates of Mdm2, wild-type MdmX RING domain and wild-type full-length MdmX were used as substrates in two independent *in vitro* ubiquitination experiments (Figures 11 and 12).

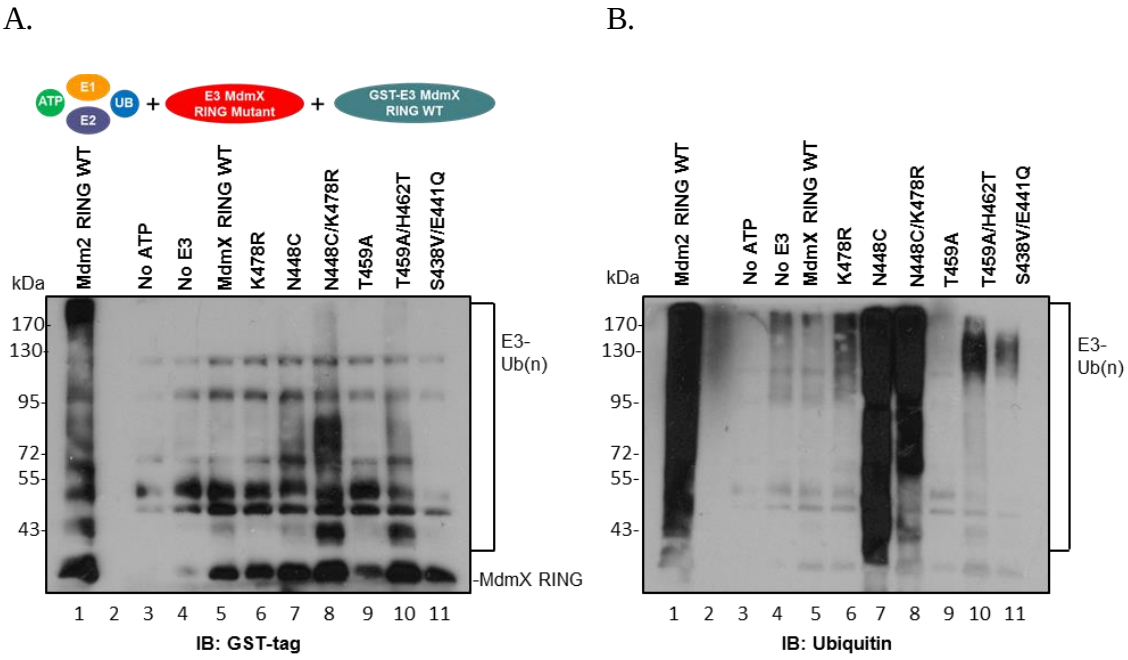

Figure 11. Ubiquitination of the wild-type MdmX RING by the mutated MdmX RING domains. The ability of the mutated MdmX RING domains to ubiquitinate wild-type MdmX RING was tested through *in vitro* ubiquitination assay which contained E1, E2 (E2D2), E3 (either His Mdm2 RING in positive and negative controls or His MdmX RING in experimental samples), ubiquitin, and ATP. Each reaction also included wild-type GST-MdmX RING to investigate substrate ubiquitination. *A*, Ubiquitination of the GST-MdmX RING domain was evaluated using a monoclonal anti-GST antibody (GE Healthcare). *B*, Substrate and autoubiquitination were detected using a monoclonal anti-ubiquitin antibody (Covance).

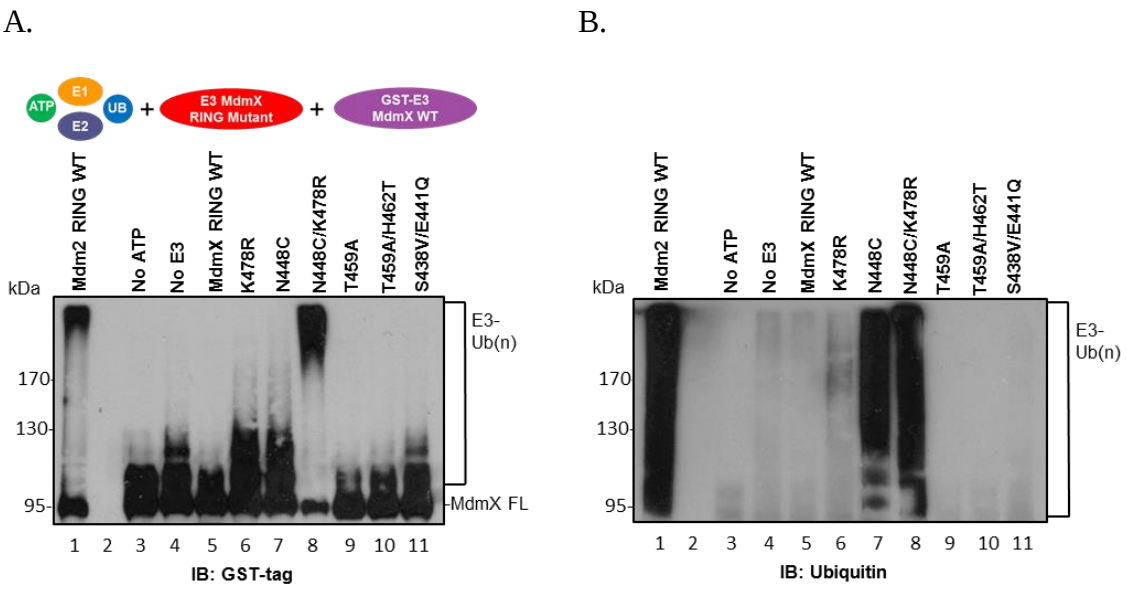

Figure 12. Ubiquitination of the wild-type full-length MdmX by the MdmX RING mutants. The ability of the mutated MdmX RING domains to ubiquitinate wild-type full-length MdmX was tested through *in vitro* ubiquitination assay which included E1, E2 (E2D2), E3 (either His Mdm2 RING in positive and negative controls or His MdmX RING in experimental samples), ubiquitin, and ATP. Each reaction also contained wild-type full-length GST-MdmX to investigate substrate ubiquitination. *A*, Ubiquitination of the full-length GST-MdmX was evaluated using a monoclonal anti-GST antibody (GE Healthcare). *B*, Substrate and autoubiquitination were detected using a monoclonal anti-ubiquitin antibody (Covance).

Ubiquitinated MdmX RING domain or full-length MdmX were detected by immunoblotting using an anti-GST tag antibody (Figures 11A and 12A). The total ubiquitinated products that are produced from both autoubiquitination activity and substrate ubiquitination were identified by immunoblotting using an anti-ubiquitin antibody (Figures 11B and 12B). As expected, Mdm2 RING domain showed a strong ability to ubiquitinate MdmX RING domain and full-length MdmX, whereas MdmX RING domain showed no ubiquitination activity. Consistent with results from the *in vitro* autoubiquitination experiments, single mutations K478R and N448C, double mutations

N448C/K478R, T459A/H462T, and S438V/E441Q showed autoubiquitination activity (Figures 11B and 12B). However, only MdmX RING N448C, N448C/K478R, and T459A/H462T mutants were able to ubiquitinate wild-type MdmX RING domain (Figure 11A). In the experiment using full-length MdmX as the substrate, only double substitution N448C/K478R allowed mutated MdmX RING domain to ubiquitinate full-length MdmX (Figure 12A). Together, the Mdm2 RING residues valine 439, glutamine 442, cysteine 449, alanine 460, threonine 463, and arginine 479 showed importance for E3 ligase activity. However, it is possible that different residues could be required for auto- or substrate ubiquitination. The Mdm2 RING domain residues cysteine 449 and arginine 479 were found to be important for ubiquitination of the full-length MdmX.

2.3.5. Structural characterization of the MdmX RING domain mutants

2.3.5.1 Analysis of the dimerization region

In this study several single and double amino acid substitutions could turn an inactive MdmX RING domain into an active E3 ligase *in vitro*, suggesting that these particular residues might be essential for the catalytic activity of an E3 ligase. Following a structural analysis of the Mdm2/MdmX RING dimerization region mainly composed of hydrophobic and small polar residues; the role of Mdm2 RING C449 and K454 in the ubiquitination reaction was examined. As shown in Figures 13 and 14, the Mdm2 RING C449 residue and the MdmX RING N448 residue reside at the same position when comparing the Mdm2 RING and MdmX RING domain monomers. However, in the dimer structure the side chains of two residues protrude into the central space of the

β-barrel from two opposite sides. As asparagine has a longer side chain than cysteine, two long polar side chains of N448 within the MdmX RING dimerization domain could position the two residues too close possibly making a negative impact on the dimer formation and stability of the MdmX RING homodimer (Figures 14A-C). However, the presence of cysteine (C449) at the same position could favour formation of the Mdm2 RING homodimer or the Mdm2/MdmX heterodimer, both of which act as active E3 ligases (Figure 13). In particular, the side chains of one cysteine (C449) and one asparagine residue (N448) in the Mdm2/MdmX RING heterodimer could form hydrogen bonding contributing to the thermodynamic stability of the heterodimer (Figures 13D-F). Similarly, a N448C substitution within the MdmX RING mutant homodimer could promote protein stability and contribute to the E3 ligase activity (Figures 14D and 14E). Importantly, a previous study showed that MdmX N448C substitution turned an inactive MdmX RING domain into an active E3 ligase for p53 *in vitro*, further supporting the important function of this residue in mediating Mdm2 E3 ligase activity (Iyappan et al., 2010).

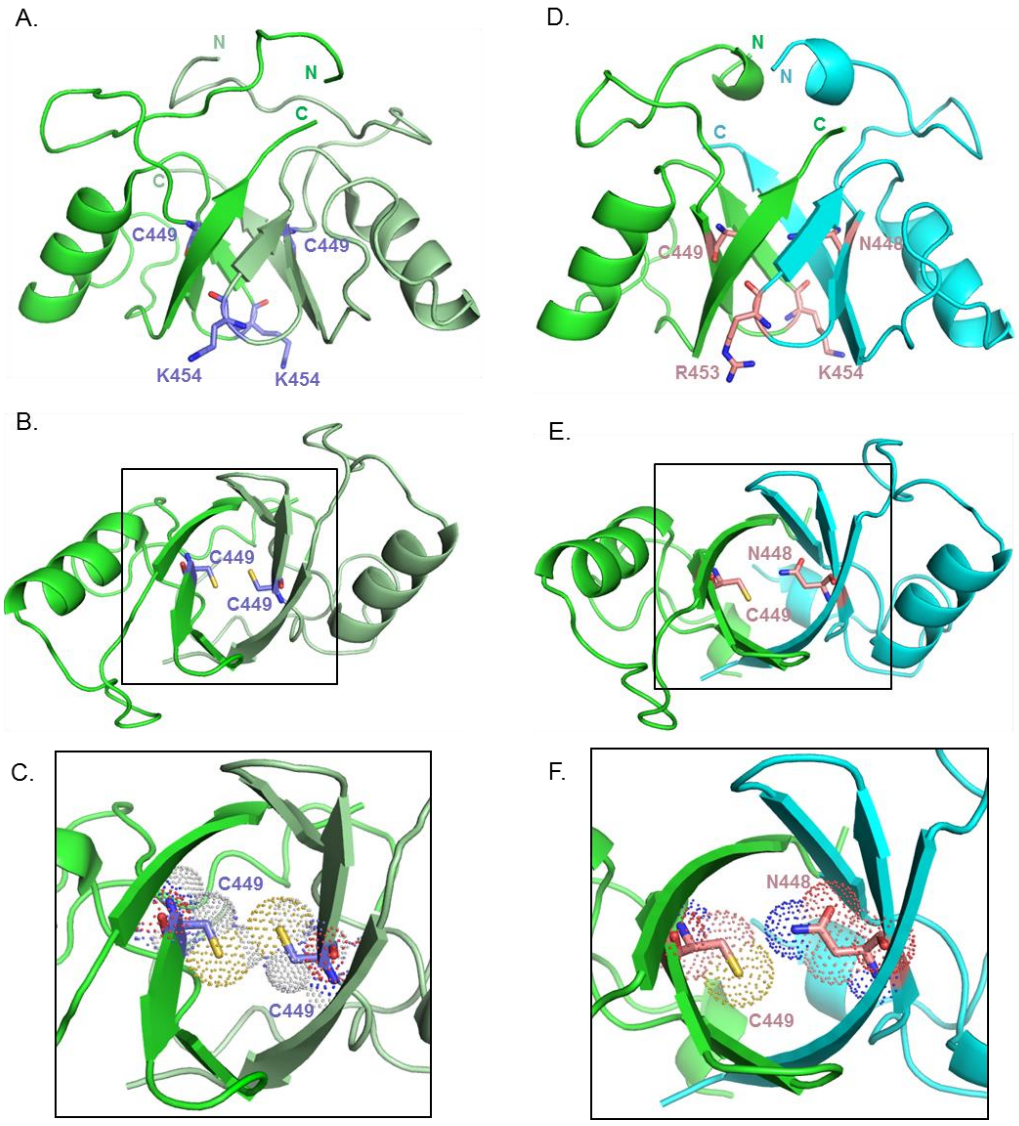

Figure 13. Structural analysis of the dimerization region of the Mdm2 RING homodimer and the Mdm2/MdmX RING heterodimer. *A*, Computer model of the Mdm2 RING domain homodimer (PDB 2HDP) is depicted. Subunit 1 is shown in green, subunit 2 – in pale green. Cysteine 449 (C449) and lysine 454 (K454) residues are highlighted in blue. N-terminus is indicated as N, and C-terminus – as C. *B*, The bottom view of the molecule is shown. *C*, The enlarged view of the dimerization region of the complex is shown. *D*, Computer model of the Mdm2/MdmX RING domain heterodimer (PDB 2VJE) is demonstrated. Mdm2 RING subunit is shown in green, MdmX RING subunit – in cyan. Mdm2 RING cysteine 449 (C449) and lysine 454 (K454) residues and MdmX RING asparagine 448 (N448) and arginine 453 (R453) are highlighted in pink. N-terminus is indicated as N, and C-terminus – as C. *E*, The bottom view of the molecule is shown. *F*, The enlarged view of the dimerization region of the complex is depicted.

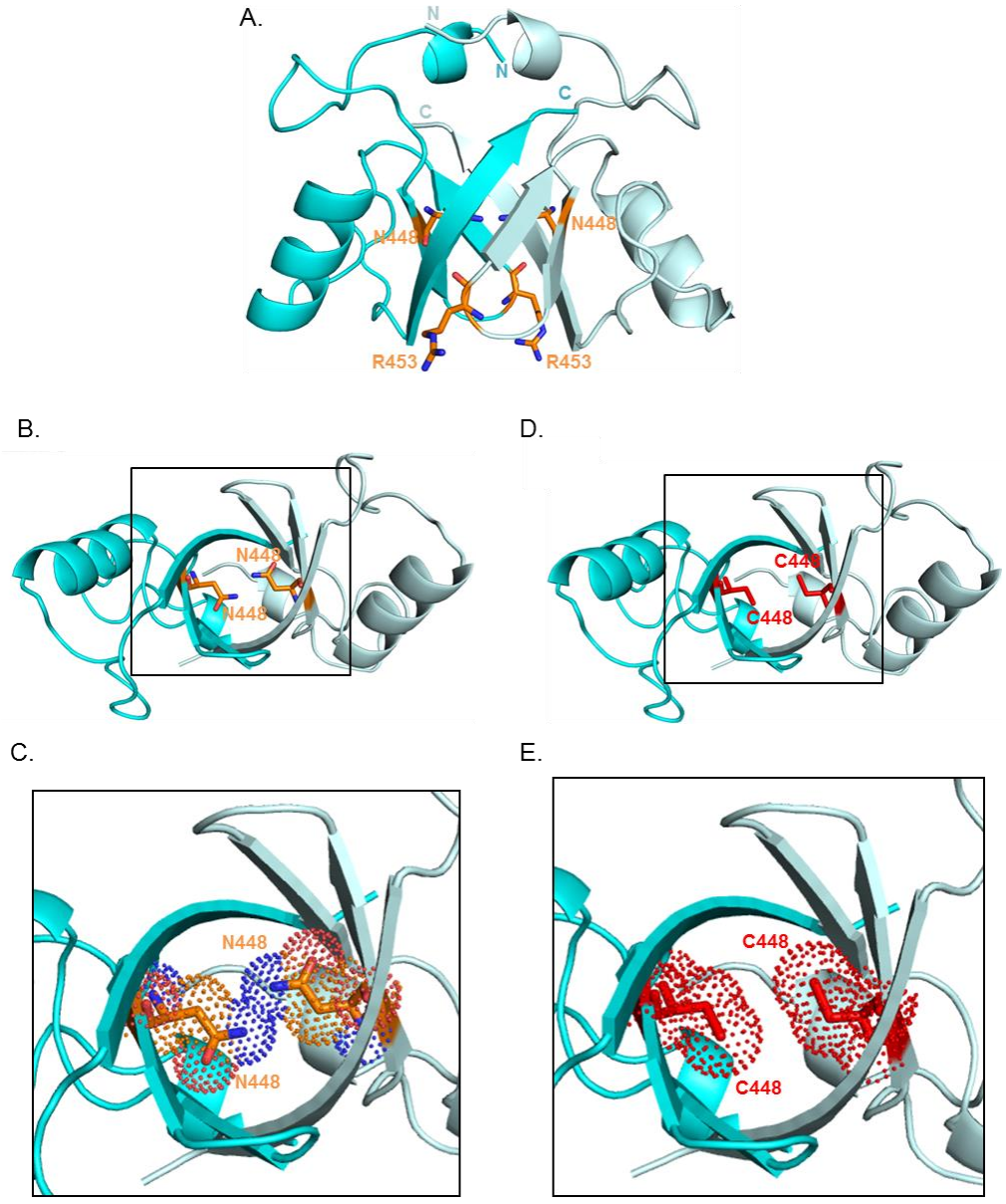

Figure 14. Structural analysis of the dimerization region of the MdmX RING homodimer. *A*, Computer model of the MdmX RING domain homodimer (PDB 2VJE) is demonstrated. Subunit 1 is shown in cyan, subunit 2 – in pale cyan. Asparagine 448 (N448) and arginine 453 (R453) residues are highlighted in orange. N-terminus is indicated as N, and C-terminus – as C. *B*, The bottom view of the molecule. *C*, The enlarged view of the dimerization region of the complex is depicted. *D*, The bottom view of the mutated MdmX RING N448C homodimer is shown. Cysteine 448 is shown in red. *E*, The enlarged view of the dimerization region of the mutated complex is demonstrated.

In addition, the role of Mdm2 RING K454 and MdmX RING R453 was investigated. In the Mdm2/MdmX heterodimer structure, both R453 and K454 are located at the dimerization interface (Figure 13D). The backbone carbonyl group of MdmX RING R453 forms a hydrogen bond with the backbone amide group of Mdm2 RING L487, and the backbone carbonyl group of Mdm2 RING K454 forms a hydrogen bond with the backbone amide group of MdmX RING K486. Their side chains do not contribute to dimerization. Previous studies have also reported mutation of Mdm2 RING K454 did not abolish the ubiquitination function of Mdm2 (Poyurovsky et al., 2003; Priest et al., 2010). The role of Mdm2 RING K454 and MdmX RING R453 was studied in the double mutant MdmX RING R453K/K478R. Even though MdmX RING K478R single mutant acquired E3 ligase activity as discussed below, MdmX RING R453K/K478R mutant showed very little effect, suggesting K454 does not contribute to E3 ligase activity of the Mdm2 RING domain.

2.3.5.2 Analysis of the E2 binding region

We also performed a structural analysis of the E2 binding surface of the Mdm2 RING domain and examined the roles of Mdm2 RING residues V439, Q442, A460, T463, R479, Q480, and P481 for E2 recruitment (Figure 15). As a result of the mutational and functional analyses of the generated MdmX RING domain mutants, we found K478R, N448C/K478R, T459A/H462T, and S438V/E441Q mutations giving MdmX RING a weak ability to perform autoubiquitination. In addition, we observed wild-type MdmX RING ubiquitination by MdmX RING K478R, N448C/K478R, and T459A/H462T, and wild-type full-length MdmX ubiquitination by MdmX RING N448C/K478R. In particular, Mdm2 RING R479 was mutated in previous studies, and its substitution abolished E3 ligase activity of Mdm2 (Linke et al., 2008; Shloush et al., 2011). The MdmX RING domain with arginine at position 478 became an active E3 ligase, presumably due to a more favourable interaction with the residue Q92 of the E2 enzyme UbcH5B (Figure 16). However, this should be confirmed with solving the structure of the MdmX RING domain mutant and an E2 enzyme. Interestingly, only MdmX RING N448C/K478R was able to perform autoubiquitination and substrates ubiquitination tested in this study. Possibly, changes within both the dimerization region and the E2 binding region were necessary for the function.

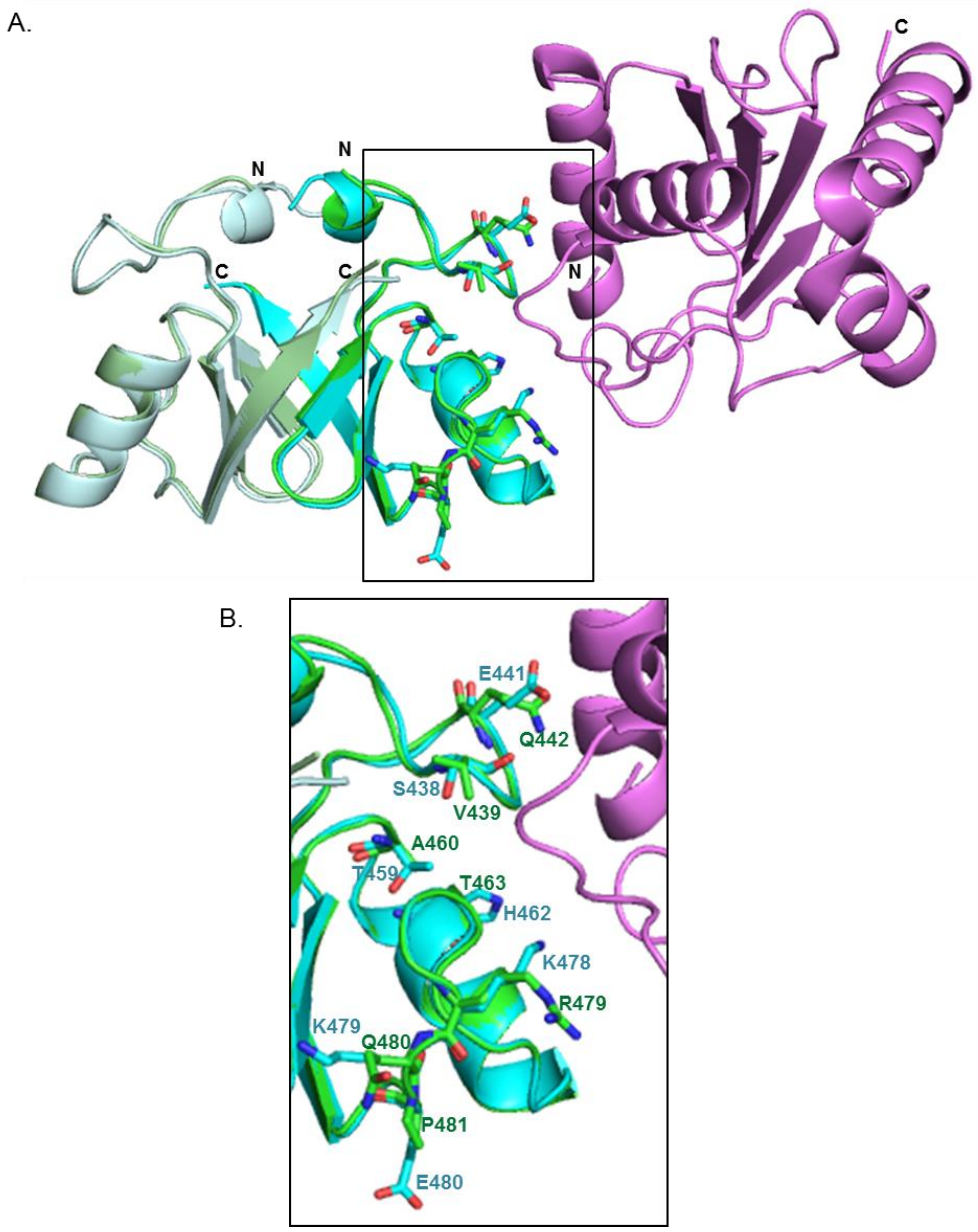

Figure 15. Structural analysis of the E2 binding surface of the Mdm2 and MdmX RING domains. *A*, Computer model of the E2-E3 complex, where the Mdm2 RING and MdmX RING homodimers are aligned (PDB 3EB6, PDB 2VJE). Mdm2 RING homodimer is shown in green/pale green, MdmX RING homodimer – in cyan/pale cyan, E2/UbcH5B – in violet. The residues of interest located at the E2 binding surface are shown in sticks. N-terminus is indicated as N, and C-terminus – as C. *B*, The enlarged view of the putative residues involved in E2 binding within the Mdm2 and MdmX RING domains is depicted. Mdm2 RING subunit is shown in green, MdmX RING subunit – in cyan. Mdm2 RING residues are indicated in green, MdmX RING residues – in cyan.

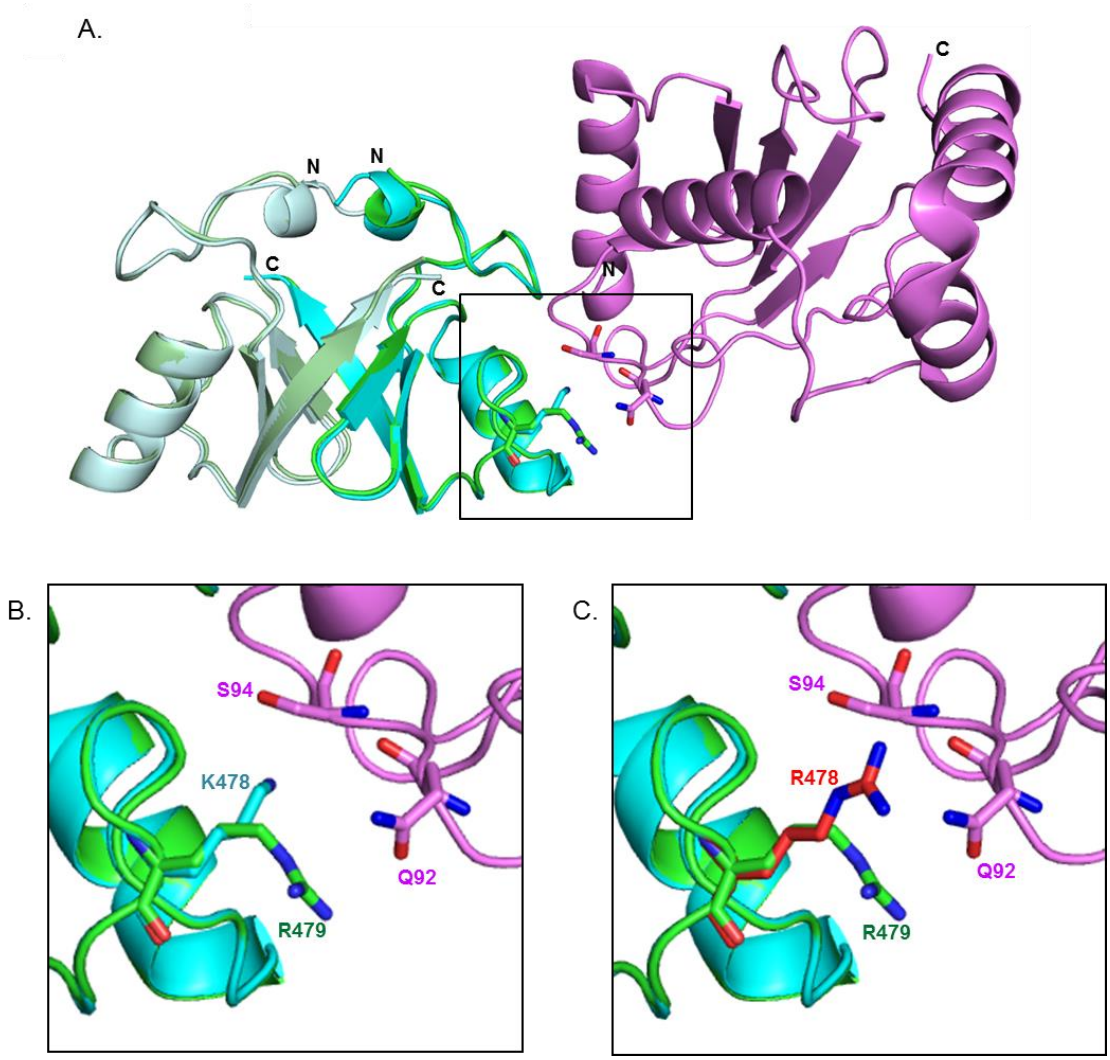

Figure 16. Structural analysis of the E2 binding surface of the Mdm2 and MdmX RING domains. *A*, Computer model of the E2-E3 complex, where the Mdm2 RING and MdmX RING homodimers are aligned (PDB 3EB6, PDB 2VJE). Mdm2 RING homodimer is shown in green/pale green, MdmX RING homodimer – in cyan/pale cyan, E2/UbcH5B – in violet. Mdm2 RING arginine 479 (R479) and MdmX RING lysine 478 (K478) are shown in sticks. N-terminus is indicated as N, and C-terminus – as C. *B*, The enlarged view of the putative interaction between the wild-type E3 and E2/UbcH5B. The molecular orientation of the Mdm2 RING R479, MdmX RING K478 and E2/UbcH5B serine 94 (S94) and glutamine 92 (Q92) is shown. *C*, The enlarged view of the putative interaction between the mutated E3 and E2/UbcH5B is demonstrated. The molecular orientation of the Mdm2 RING R479, MdmX RING R478 (shown in red) and E2/UbcH5B S94 and Q92 is shown.

Previously, Mdm2 RING V439 and Q442 were mutated to alanine, and these substitutions were not found to abolish Mdm2 autoubiquitination activity (Linke et al., 2008). However, another study showed Q442 mutation to alanine was able to block both Mdm2 autoubiquitination and p53 ubiquitination (Shloush et al., 2011). Our present finding showed that MdmX RING S438V/E441Q mutant gained ability to ubiquitinate itself, but not the substrate, suggesting its role in autoubiquitination.

Finally, MdmX RING T459A/H462T mutant, located within the central helix, acquired very weak ubiquitination activity possibly due to H462T mutation since MdmX RING T459A did not show E3 ligase activity. The neighboring Mdm2 RING T463A was previously shown to possess wild-type ubiquitination activity suggesting this residue is dispensable in the ubiquitination reaction (Shloush et al., 2011). Therefore, these residues located within the central helix likely do not play an essential role in the Mdm2 E3 ligase activity.

2.4. Discussion

In this study, structural and functional analyses of the Mdm2 RING domain were performed to further explore and characterize its active site. Specifically, a number of residues within the Mdm2/MdmX dimerization surface and the E2 binding surface of the Mdm2 RING domain were selected and introduced into the MdmX RING domain at the corresponding sites. Considering MdmX lacked intrinsic E3 ligase activity, in case the mutation resulted in the MdmX RING domain gaining ubiquitination activity, the residues were considered to be critical for Mdm2 RING-mediated E3 ligase function.

Maintenance of the proper functioning of Mdm2 as a ubiquitin ligase depends on two aspects: 1) dimerization with itself or MdmX via their RING domains, and 2) recruitment of an E2 ubiquitin conjugating enzyme. The core of the RING domain dimer is composed of two β-sheets, one from each subunit. In turn, each β-sheet consists of three β-strands. Mostly hydrophobic and small polar amino acid residues are located within this region. In this study, Mdm2 RING C449 located within the β1-strand and K454 located within the loop region connecting β1-strand and β2-strand were investigated and tested for their potential roles in dimerization and ubiquitination activity. C449 was found to participate in E3 ligase function. Similarly, C449 was demonstrated to be involved in the Mdm2 RING-mediated ubiquitination process in an independent investigation (Iyappan et al., 2010). Previous studies used mutagenesis and deletion experiments to show the importance of the C-terminal β3-strand for the Mdm2 RING-mediated E3 ligase activity and dimerization (Poyurovsky et al., 2007; Shloush et al., 2010). Furthermore, this study aimed to expand the existing knowledge on the E2 recruitment surface and its importance for the ubiquitination activity. Amino acid residues located within the loop regions and the α-helix were observed to be potentially involved in the formation of the E2-E3 interactions. A number of the RING domain residues were tested, and their roles in E3 ligase activity were found consistently with previous studies (Linke et al., 2008; Shloush et al., 2010). Together, these findings confirmed the significance for maintaining integrity of the hydrophobic core of the Mdm2 RING domain and the E2 binding region for its E3 ligase activity.

Moreover, from our findings we observed more MdmX RING domain mutants were capable of performing autoubiquitination than substrate ubiquitination. This could mean that differential involvement of the amino acid residues could take place depending on the type of ubiquitination reaction occurring and the substrate. Structural and biochemical analyses of the Mdm2 RING domain supporting this notion are lacking. However, certain conclusions might be drawn from the cell-based assays investigating small molecule inhibitors of the Mdm2 RING E3 ligase activity. A number of chemical compounds were observed to inhibit Mdm2 autoubiquitination, or p53 ubiquitination, or both (Dickens et al., 2010). To restore p53 level and function in tumour cells a potent compound would have to specifically inhibit Mdm2-mediated p53 ubiquitination, while allowing Mdm2 autoubiquitination. Therefore, it seems essential to further investigate the Mdm2 RING residues responsible for autoubiquitination and substrate ubiquitination.

This study provided a further insight into the Mdm2 RING-mediated ubiquitin transfer mechanism providing more knowledge for the structure-assisted design of anti-cancer compounds targeting E3 ligase activity of Mdm2 in malignant cells.

CHAPTER 3: A comparative analysis of the human Mdm2 and MdmX RING domain functions *in vivo*

3.1. Introduction

Post-translational modifications play a crucial role in modulation of p53 fate and function. In particular, phosphorylation of the N-terminal domain and acetylation of the C-terminal domain have been denoted as markers of the activated p53 (Brooks and Gu, 2010; Gu and Roeder, 1997). Mdm2-mediated ubiquitination can either destine p53 for nuclear export or proteasomal degradation (Marchenko et al., 2007; Brooks et al., 2004; Haupt et al., 1997; Honda et al., 1997; Kubbutat et al., 1997). In both cases transcription activity of p53 becomes suppressed. Mdm2-dependent p53 degradation is one of the major mechanisms of maintaining low p53 level in absence of stress; therefore, Mdm2 is considered the main negative regulator of p53 (Honda et al., 1997).

Mdm2-mediated inhibition of the function of p53 as a tumour suppressor is facilitated by two major ways: inhibition of transcriptional activation and ubiquitination of p53 (Chen et al., 1995; Momand et al., 1992). It is critical to mention that the *MDM2* gene promoter is under transcriptional control of p53 (Wu et al., 1993). Therefore, an increasing cellular level of p53 triggers an increase in Mdm2 expression, which in turn acts to downregulate p53, thereby, placing p53 and Mdm2 in a negative feedback loop (Wu et al., 1993). In addition to p53 ubiquitination, Mdm2 can ubiquitinate other substrates, such as itself or MdmX (Pan and Chen, 2003; Fang et al., 2000). These functions are attributed to the RING domain, which mediates Mdm2/Mdm2 homodimer

or Mdm2/MdmX heterodimer formation and catalyzes ubiquitin transfer (Fang et al., 2000; Tanimura et al., 1999).

MdmX, or Murine Double Minute X, is homologous to Mdm2 in structure and function and is another important negative regulator of p53 (Shvarts et al., 1996; Shvarts et al., 1997). Similar to Mdm2, MdmX can interact with p53 via their N-terminal domains and inhibit p53 gene transcription activity (Bottger et al., 1999). Unlike Mdm2, MdmX RING lacks ubiquitination activity making MdmX an inactive E3 ligase; however, MdmX possesses an ability to stabilize Mdm2 through heterodimerization mediated by the RING domains (Sharp et al., 1999; Stad et al., 2001; Tanimura et al., 1999).

Gene amplification and overexpression of Mdm2 and MdmX have been associated with many types of human malignancies (Wade et al., 2010). Aberrant splice variants of the *MDM2* and *MDMX* genes have been identified from aggressive forms of cancers. However, the origin and the functions of these splice variants remain poorly understood. For instance, MDM2-A and $HDM2^{ALT1}$ are the *MDM2* gene products characterized as lacking the N-terminal p53 binding domain, however, containing the complete C-terminal RING domain (Evans et al., 2001; Volk et al., 2009). On one hand, they were found to interact with Mdm2 *in vivo* through dimerization. Acting as a dominant negative form, these Mdm2 RING domain variants disrupt Mdm2-dependent suppression of p53 function (Evans et al., 2001; Volk et al., 2009). On the other hand, murine forms of the Mdm2 splice variants containing an intact RING domain demonstrated the oncogenic

effect in a mouse model showing accelerated cancer progress (Fridman et al., 2003). Moreover, *MDMX* gene splice variant, HDMX211, missing an N-terminal p53 binding domain, but containing an intact C-terminal RING domain was also identified. Similar to Mdm2 RING domain variants, it was shown to interact and inhibit the ability of Mdm2 to target p53 for degradation (Giglio et al., 2005). However, these studies have not elucidated the mechanisms of action of these Mdm2 and MdmX splice variants. Here, a comprehensive study is performed to characterize the functions of the Mdm2 and MdmX RING domains and their effects on p53 stabilization and transactivation in a human osteosarcoma U2OS cell line.

3.2. Materials and Methods

3.2.1. Plasmids

Human full-length Mdm2 (FL), full-length MdmX (FL), Mdm2 RING (residues 417-491), and MdmX RING (residues 416-490) domains were cloned into pcDNA3.1/YFP, pcDNA3.1/CFP, and pc-DNA3.1/FLAG expression vectors using a standard PCR technique.

3.2.2. Cell culture and transfection

Human osteosarcoma U2OS cells were grown in McCoy's medium supplemented with 10% FBS. Cells were transfected with plasmids (10 ug of DNA per 10 cm tissue culture plate) using PolyJet transfection reagent (SignaGen Laboratories).

3.2.3. Antibodies

The antibodies for immunoblotting and co-immunoprecipitation were mouse monoclonal against Mdm2 (Santa Cruz SMP14, sc-965), MdmX (Millipore 8C6, 04-1555), p53 (Santa Cruz DO-1, sc-126), actin (Santa Cruz C-2, sc-8432), GAPDH (Santa Cruz 0411, sc-47724), YFP-tag (Abm G163), FLAG-tag (Sigma F3165), rabbit monoclonal against phosphorylated p53 (serine 15) (Cell Signaling #9284), p21 (Santa Cruz C-19, sc-397), Bax (Cell Signaling #2772), and rabbit polyclonal against FLAG-tag (Bethyl Laboratories A190-102A). To detect proteins of interest HRP-conjugated anti-mouse IgG (Jackson ImmunoResearch 115-035-166) and anti-rabbit IgG (Jackson ImmunoResearch 111-035-003) antibodies were used.

3.2.4. Immunoblotting

U2OS cells were transfected with YFP (empty vector), CFP-Mdm2 FL, CFP-MdmX FL, YFP-Mdm2 RING, and YFP-MdmX RING or FLAG (empty vector), FLAG-Mdm2 FL, FLAG-MdmX FL, FLAG-Mdm2 RING, and FLAG-MdmX RING. Cells were harvested 24 hours post-transfection and lysed in radioimmunoprecipitation buffer (50 mM Tris-HCl pH 8.0, 150 mM NaCl, 0.5% Nonidet P-40, 1X protease inhibitor cocktail (Roche)) followed by 2 sec sonication time with 10% amplitude. Supernatants (100 ug of total protein) were boiled in SDS sample buffer for 5 minutes at 95^{o}C. Samples were resolved on 12% or 7.5% SDS-PAGE, and immunoblotting was performed using antibodies described above.

3.2.5. Fluorescent microscopy

U2OS cells were transfected with CFP-Mdm2 FL, CFP-MdmX FL, YFP-Mdm2 RING, and YFP-MdmX RING and grown on coverslips. 24 hours post-transfection cells were fixed in 1% paraformaldehyde in PBS and permeabilized with 0.5% Triton-X in PBS. Cells were washed with PBS two times. Images were obtained using Zeiss LSM 700 Laser Scanning microscope and LSM software ZEN2010.

3.2.6. Co-immunoprecipitation

U2OS cells were transfected with CFP-Mdm2 FL and either FLAG-Mdm2 RING or FLAG-MdmX RING; CFP-MdmX FL and either FLAG-Mdm2 RING or FLAG-MdmX RING to detect protein-protein interactions. Cells were harvested 24 hours post-transfection and lysed in radioimmunoprecipitation buffer (50 mM Tris-HCl pH 8.0, 150 mM NaCl, 0.5% Nonidet P-40, 1X protease inhibitor cocktail (Roche)) followed by 2 sec sonication time with 10% amplitude. Cell lysates were incubated with a rabbit polyclonal anti-FLAG tag primary antibody for 2 hours followed by addition of pre-cleared protein A/G Plus-Agarose beads (Santa Cruz, sc-2003) for 1 hour. Immunoprecipitates were washed with radioimmunoprecipitation buffer three times and then boiled in SDS sample buffer for 5 minutes at 95^{o}C to release protein complexes from the beads. Samples were resolved on 12% SDS-PAGE, and immunoblotting was performed using antibodies described above.

3.3. Results

3.3.1. Ectopic expression of the Mdm2 and MdmX RING domains in U2OS cells

To study functions of the Mdm2 and MdmX RING domains *in vivo*, Mdm2 and MdmX RING domains were ectopically expressed as YFP/CFP or FLAG-tagged fusion proteins in U2OS cells. Full-length wild-type Mdm2 and MdmX were expressed as positive controls. Exogenous protein expression was determined with immunoblotting using antibodies against a YFP-tag or a FLAG-tag (Appendix B. Figures 5 and 6). YFP-Mdm2 RING and YFP-MdmX RING were detected around 35 kDa (Appendix B. Figures 5A and 5B, lanes 4 and 6). CFP-MdmX FL was detected around 130 kDa mark (Appendix B. Figures 5A and 5B, lane 5). Longer exposure was required to detect CFP-Mdm2 FL at a high molecular weight mark (Appendix B. Figure 5B, lane 3), suggesting that the full-length Mdm2 was less stable than other ectopically expressed constructs. Similar expression pattern was observed for FLAG-Mdm2 FL, FLAG-MdmX FL, FLAG-Mdm2 RING and FLAG-MdmX RING (Appendix B. Figures 6A and 6B).

3.3.2. Effect of the ectopic Mdm2 and MdmX RING domains on the cellular levels of Mdm2 and MdmX

To characterize functions of the ectopically expressed Mdm2 and MdmX RING domains *in vivo*, cellular levels of the endogenous Mdm2 and MdmX were determined by immunoblotting in U2OS cells as the effect of the overexpressed Mdm2 and MdmX RING domains and compared to the effect of the overexpressed full-length wild-type Mdm2 (Mdm2 FL) and MdmX (MdmX FL) (Figure 17).

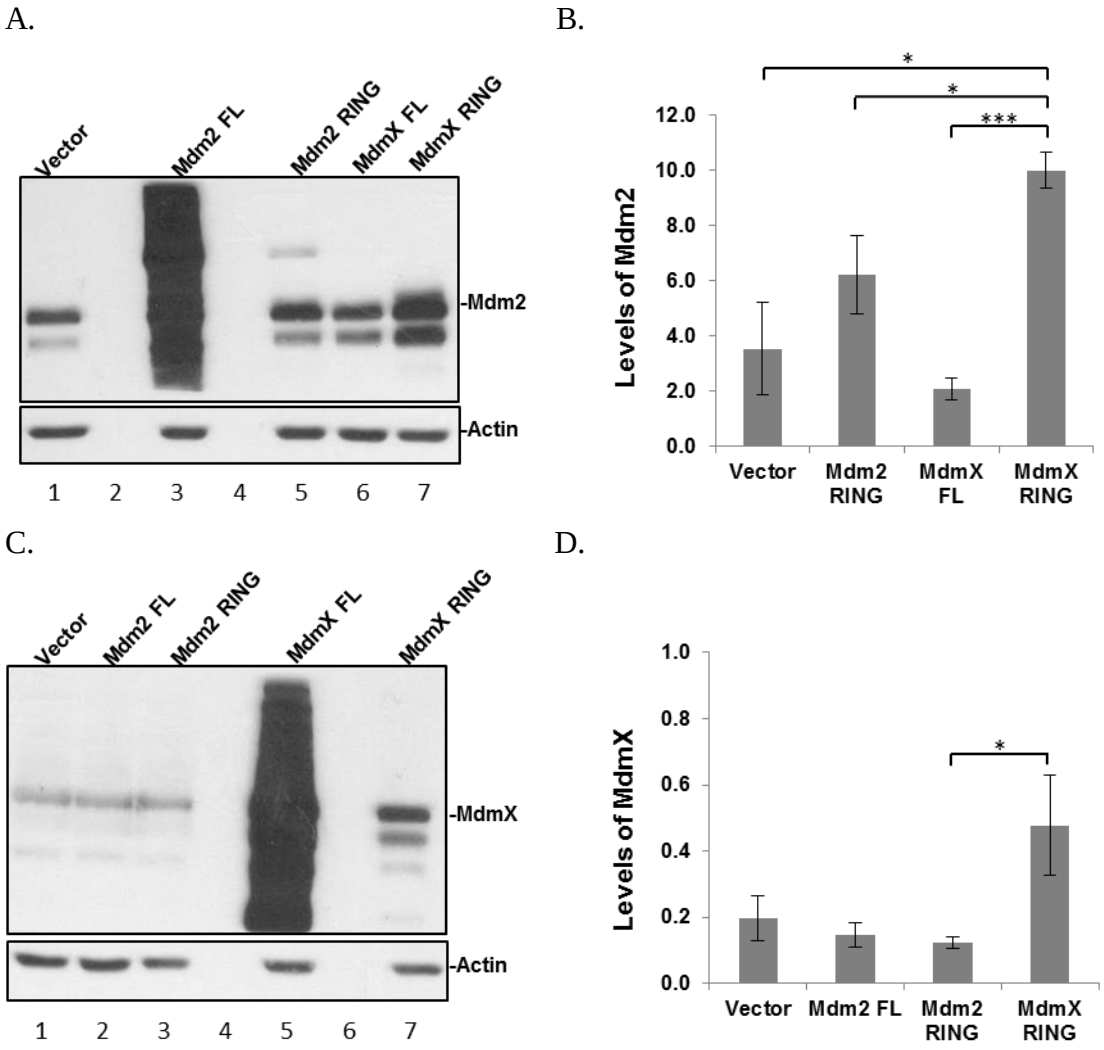

Figure 17. Effect of the ectopically expressed Mdm2 RING and MdmX RING on the endogenous Mdm2 and MdmX. Wild-type full-length Mdm2 and MdmX were expressed as CFP-fusion proteins; Mdm2 and MdmX RING were expressed as YFP-fusion proteins. U2OS cells were transfected with an empty YFP vector, CFP-Mdm2, CFP-MdmX, YFP-Mdm2 RING, and YFP-MdmX RING. Protein samples were prepared 24 hours post-transfection. *A* and *C*, Immunoblotting was carried out with monoclonal anti-Mdm2 (1:500), anti-MdmX (1:500), and anti-Actin (1:5000) (loading control) antibodies. *B* and *D*, Quantitative analysis of the level of the endogenous Mdm2 and MdmX is shown. Data are represented as means $\pm$ SEM (n=3) with * $p<0.05$ and *** $p<0.001$.

A smear was observed in the lane with ectopic expression of CFP-Mdm2 (Figure 17A, lane 3); therefore, it was not possible to evaluate cellular level of the endogenous Mdm2. However, no significant effect was revealed with an overexpression of FLAG-Mdm2 FL where an upper band corresponded to the exogenous Mdm2, and a lower band represented the endogenous Mdm2 (Figure 20A). Overexpression of MdmX FL resulted in a mild decrease of the endogenous level of Mdm2 (Figure 17A, lane 6). Ectopically expressed Mdm2 RING led to a mild increase of the Mdm2 level (Figure 17A, lane 5), whereas overexpressed MdmX RING resulted in a significant increase of the Mdm2 level (Figure 17A, lane 7).

The effect on the endogenous MdmX was shown in Figures 17C and 17D. Ectopic expression of Mdm2 FL or Mdm2 RING did not have effects on the endogenous MdmX levels (Figure 17C, lanes 2, 3). Due to high levels of the ectopically expressed MdmX FL masking the endogenous MdmX level, the effect of the ectopic overexpression of MdmX FL on the endogenous MdmX was not determined (Figure 17C, lane 5). Interestingly, overexpression of MdmX RING led to an increase in the endogenous MdmX level. Consistent results were obtained with the overexpressed Mdm2 and MdmX proteins tagged with FLAG (Figure 20B).

Collectively, Mdm2 and MdmX RING demonstrated a different effect on the endogenous Mdm2 and MdmX. MdmX RING domain stabilized both Mdm2 and MdmX, but Mdm2 RING domain had little effect.

3.3.3. Effect of the ectopic Mdm2 and MdmX RING domains on the cellular levels of p53

The effect of ectopic expression of the Mdm2 and MdmX full-length and RING domains on the level of p53 itself was examined (Figures 18A and 18B). A significant decrease of p53 was found following overexpression of Mdm2 FL (Figure 18A, lane 2). Only a slight increase in p53 level was promoted by ectopically expressed MdmX FL (Figure 18A, lane 4). Finally, overexpression of Mdm2 RING and MdmX RING did not lead to a significant change in the endogenous p53 levels (Figure 18A, lanes 3, 5). The results of this experiment showed that ectopic expression of Mdm2 RING and MdmX RING did not affect stabilization of p53 in cells in contrast to overexpression of Mdm2 FL and MdmX FL that demonstrated a negative and a positive effect on the cellular p53 stability, respectively. Similar results were obtained using FLAG-fusion exogenous proteins (Figure 21A).

3.3.4. Effect of the ectopic Mdm2 and MdmX RING domains on the transcriptional activity of p53 in vivo

To further characterize functions of the ectopically expressed Mdm2 RING and MdmX RING domains in U2OS cells, gene transcription activity of p53 was analyzed. First, the phosphorylation state of p53 was investigated, and then the expression of the p53 target genes was determined using immunoblotting.

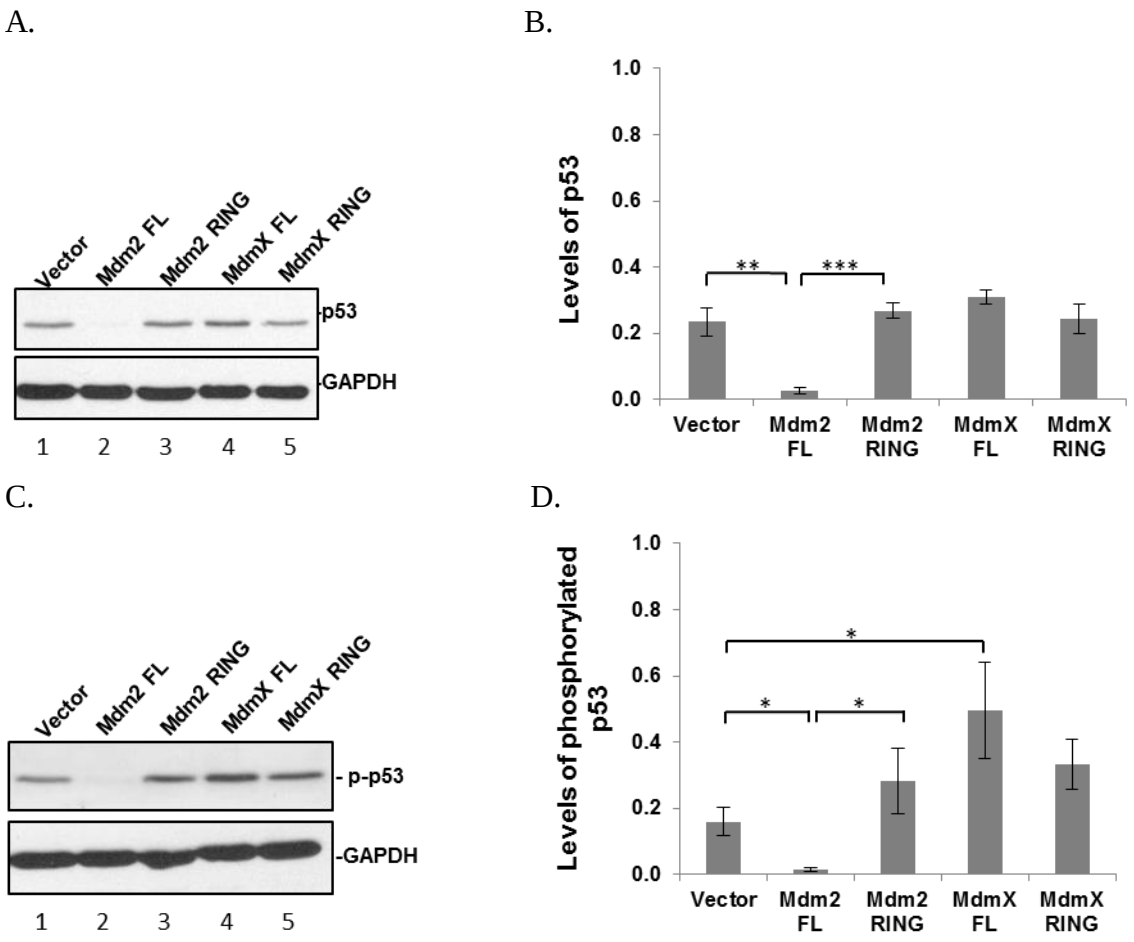

Figure 18. Effect of the ectopically expressed Mdm2 RING and MdmX RING on the endogenous p53 and phosphorylated p53. Wild-type full-length Mdm2 and MdmX were expressed as CFP-fusion proteins; Mdm2 and MdmX RING were expressed as YFP-fusion proteins. U2OS cells were transfected with an empty YFP vector, CFP-Mdm2, CFP-MdmX, YFP-Mdm2 RING, and YFP-MdmX RING. Protein samples were prepared 24 hours post-transfection. *A* and *C*, Immunoblotting was carried out with monoclonal anti-p53 (1:1000), anti-phospho-Ser15-p53 (1:500), and anti-GAPDH (1:5000) (loading control) antibodies. *B* and *D*, Quantitative analysis of the level of endogenous p53 and phosphorylated p53 is shown. Data are represented as means $\pm$ SEM (n=3) with * $p<0.05$, ** $p<0.01$, and *** $p<0.001$.

It is well-known that external stress stimuli, such as DNA damage, stabilize and activate p53, which in turn upregulates or downregulates transcription of its target genes. Activation of p53 is achieved through post-translational modifications such as phosphorylation and acetylation (Gu and Roeder, 1997; Jamal and Ziff, 1995). In this study, level of the phosphorylated p53 at serine 15 as a marker of the activated state of p53 was examined (Figures 18C and 18D). Mdm2 FL overexpression led to a decrease in the phosphorylated p53 level, whereas overexpression of MdmX FL resulted in an increase of the phosphorylated p53 (Figure 18C, lanes 2, 4). Overexpressed Mdm2 RING and MdmX RING caused a mild increase in the phosphorylated p53 levels. In agreement with the previous experiment involving analysis of the endogenous p53 level, Mdm2 FL led to p53 destabilization. In contrast, MdmX FL, Mdm2 RING, and MdmX RING contributed to a stabilization of the phosphorylated p53 suggesting different mechanisms of regulation of the active and inactive p53 in cells.

To further elucidate the effects of the ectopically expressed Mdm2 RING and MdmX RING domains on the transcriptional activity of p53, the expression of its downstream target genes was analyzed. In this study, p53-mediated expression of p21 involved in regulation of the cell cycle progression and a pro-apoptotic Bax protein was investigated (Selvakumaran et al., 1994; el-Deiry et al., 1993) (Figure 19). Overexpression of Mdm2 FL and MdmX FL led to a decrease in p21 levels (Figure 19A, lanes 2, 4). However, overexpression of Mdm2 RING and MdmX RING did not lead to a significant alteration in p21 levels (Figure 19A, lanes 3, 5). Furthermore, no changes were observed in Bax as a result of overexpression of the exogenous proteins (Figure 19C, lanes 2, 3, 4, 5). These

findings showed destabilization of p21 caused by overexpression of either Mdm2 FL or MdmX FL, but not the RING domains. Moreover, no effect on Bax protein level implied various cellular processes being recruited under ectopic expression of Mdm2 FL, MdmX FL, and their RING domains.

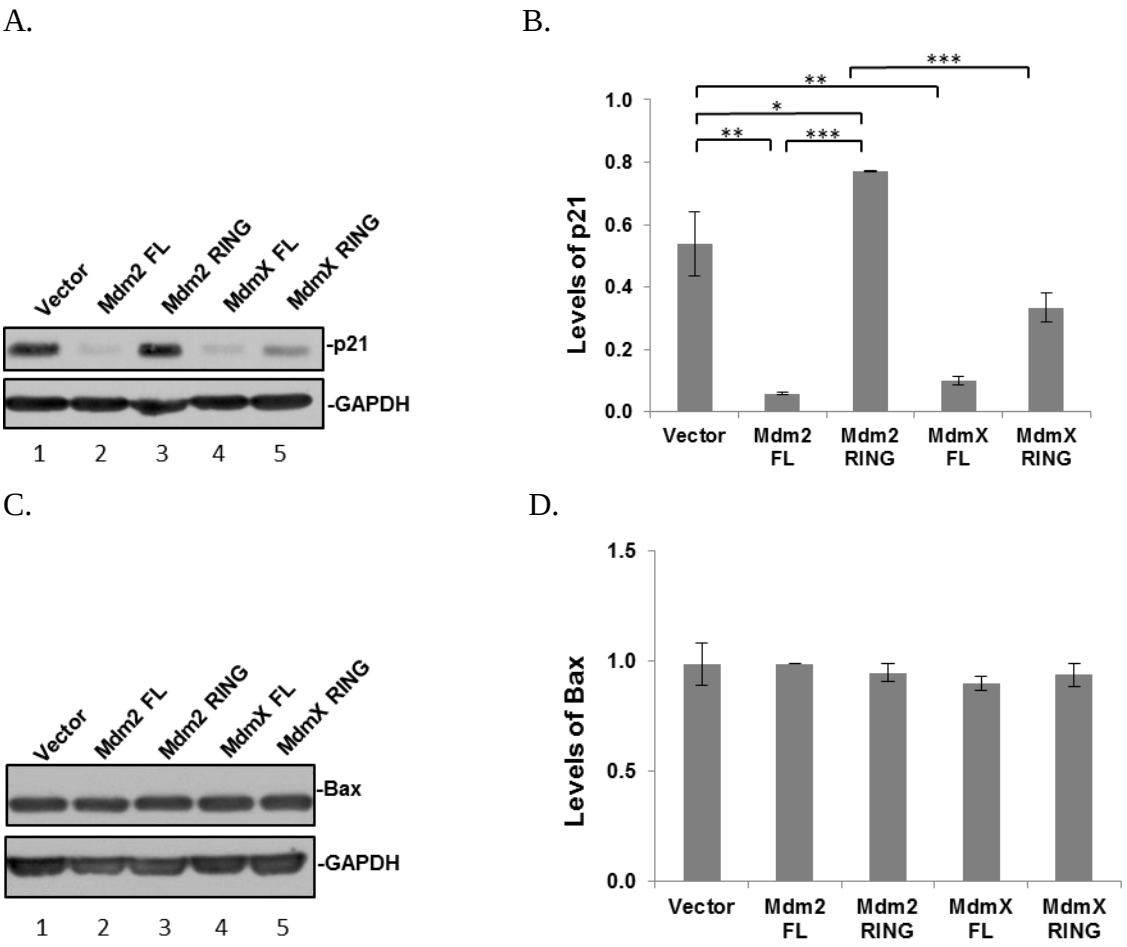

Figure 19. Effect of the ectopically expressed Mdm2 RING and MdmX RING on the endogenous p21 and Bax. Wild-type full-length Mdm2 and MdmX were expressed as CFP-fusion proteins; Mdm2 and MdmX RING were expressed as YFP-fusion proteins. U2OS cells were transfected with an empty YFP vector, CFP-Mdm2, CFP-MdmX, YFP-Mdm2 RING, and YFP-MdmX RING. Protein samples were prepared 24 hours post-transfection. *A* and *C*, Immunoblotting was carried out with monoclonal anti-p21 (1:500), anti-Bax (1:1000), and anti-GAPDH (1:5000) (loading control) antibodies. *B* and *D*, Quantitative analysis of the level of endogenous p21 and Bax is shown. Data are represented as means $\pm$ SEM (n=3) with * $p<0.05$, ** $p<0.01$, and *** $p<0.001$.

3.3.5. Effect of the ectopic Mdm2 and MdmX RING domains on the cellular levels of p53 and its negative regulators under DNA damage conditions

Both Mdm2 and MdmX are actively involved in the DNA repair signaling pathway through p53. Therefore, the effect of the ectopically expressed Mdm2 and MdmX RING domains on the endogenous levels of Mdm2 and MdmX were tested under DNA damage induced by doxorubicin, an inhibitor of DNA topoisomerase II (Figure 20). In presence of doxorubicin treatment, overexpression of Mdm2 RING domain did not show any effect on either endogenous Mdm2 or MdmX levels (Figures 20A and 20B, lane 8). However, ectopic expression of the MdmX RING domain resulted in a decreased Mdm2 level, but an increased MdmX level (Figure 20A and 20B, lane 10). Various effects of the ectopically expressed Mdm2 and MdmX RING domains on the cellular Mdm2 and MdmX implied different modes of action of these two RING domains in presence or absence of stress stimuli.

A.

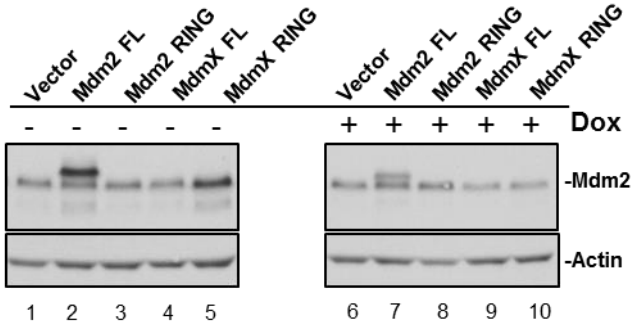

B.

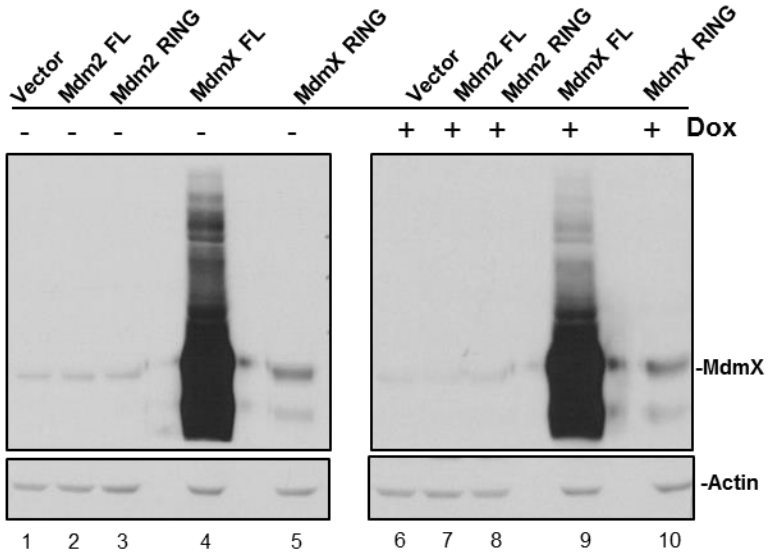

Figure 20. Effect of the ectopically expressed Mdm2 RING and MdmX RING on the endogenous Mdm2 and MdmX under stress conditions. Wild-type full-length Mdm2 and MdmX, Mdm2 RING and MdmX RING domains were expressed as FLAG-fusion proteins. U2OS cells were transfected with an empty FLAG vector, FLAG-Mdm2, FLAG-MdmX, FLAG-Mdm2 RING, and FLAG-MdmX RING. Protein samples were prepared 24 hours post-transfection and treated with 500 ng/ml of doxorubicin for 4 hours. *A* and *B,* Immunoblotting was carried out with monoclonal anti-Mdm2 (1:500), anti-MdmX (1:500), and anti-Actin (1:1000) (loading control) antibodies.

DNA-damaging signals are known to cause stabilization of the cellular p53 and activation of its gene transcription activity. As expected, an overall significant increase in cellular levels of the unphosphorylated and phosphorylated p53 was observed following doxorubicin treatment compared to no treatment (Figure 21). Regardless of presence of stress conditions, overexpression of Mdm2 FL led to a decrease in p53 level (Figure 21A and 21B, lane 7). Ectopically expressed MdmX FL, or the RING domains did not affect p53 levels (Figure 21A and 21B, lanes 8, 9, 10).

A.

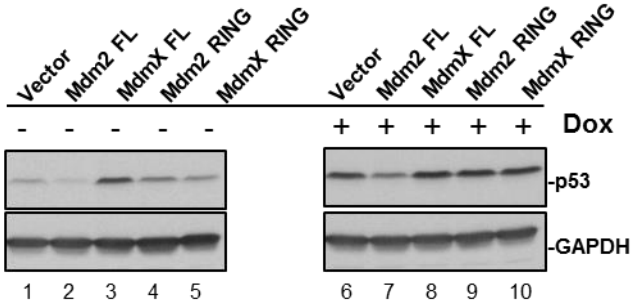

B.

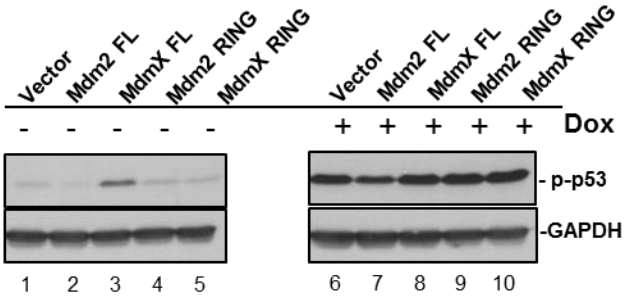

Figure 21. Effect of the ectopically expressed Mdm2 RING and MdmX RING on the endogenous p53 and phosphorylated p53 under stress conditions. Wild-type full-length Mdm2 and MdmX, Mdm2 RING and MdmX RING domains were expressed as FLAG-fusion proteins. U2OS cells were transfected with an empty FLAG vector, FLAG-Mdm2, FLAG-MdmX, FLAG-Mdm2 RING, and FLAG-MdmX RING. Protein samples were prepared 24 hours post-transfection and treated with 500 ng/ml of doxorubicin for 4 hours. *A* and *B*, Immunoblotting was carried out with monoclonal anti-p53 (1:1000), anti-phospho-Ser15-p53 (1:1000), and anti-GAPDH (1:10000) (loading control) antibodies.

To evaluate gene transcription activity of the stabilized p53, p21 and Bax protein levels were determined in presence of a DNA-damaging signal. Following doxorubicin treatment no significant change and an increase in p21 levels was observed in samples with overexpressed Mdm2 FL and Mdm2 RING, respectively (Figure 22A, lanes 7, 8). A slight decrease in p21 was found in MdmX FL and MdmX RING samples (Figure 22A, lanes 9, 10). Lastly, under stress conditions no significant changes in Bax protein levels were detected (Figure 22B). Together, these results suggested that even though p53 was stabilized in presence of doxorubicin, it was not transcriptionally active to induce significant increases in expression of its target genes.

A.

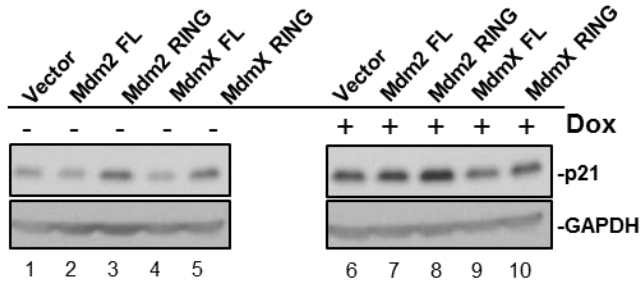

B.

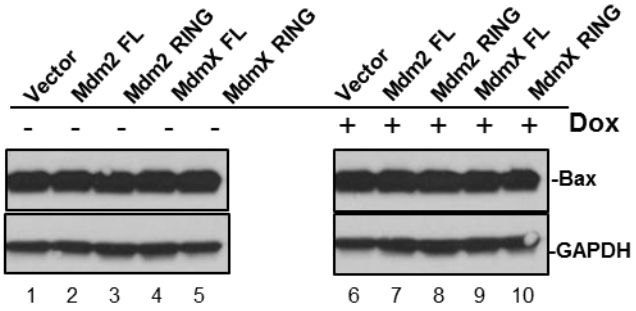

Figure 22. Effect of the ectopically expressed Mdm2 RING and MdmX RING on the endogenous p21 and Bax under stress conditions. Wild-type full-length Mdm2 and MdmX, Mdm2 RING and MdmX RING domains were expressed as FLAG-fusion proteins. U2OS cells were transfected with an empty FLAG vector, FLAG-Mdm2, FLAG-MdmX, FLAG-Mdm2 RING, and FLAG-MdmX RING. Protein samples were prepared 24 hours post-transfection and treated with 500 ng/ml of doxorubicin for 4 hours. *A* and *B,* Western blots were carried out with monoclonal anti-p21 (1:1000), anti-Bax (1:1000), and anti-GAPDH (1:10000) (loading control) antibodies.

3.3.6. Cellular localization of the ectopically expressed Mdm2 and MdmX RING domains in U2OS cells

To investigate cellular localization of the ectopically expressed Mdm2 RING and MdmX RING and further characterize their functions, U2OS cells were transfected with protein constructs carrying fluorescent tags CFP-Mdm2 FL, CFP-MdmX, YFP-Mdm2 RING, and YFP-MdmX RING (Figure 23). Mdm2 FL and MdmX overexpression served as a positive control. Nuclei were stained with DAPI for visualization.

Consistent with previous studies, Mdm2 FL was found within the nucleus, and MdmX FL was localized primarily in the cytoplasm; however, a certain amount of MdmX FL was observed in the nucleus. Interestingly, Mdm2 RING and MdmX RING domains were detected in the cytoplasm and the nucleus. Nuclear localization of Mdm2 was previously reported, and transport between the nucleus and the cytoplasm was enabled due to its nuclear localization signal and nuclear export sequence (Tao and Levine, 1999; Roth et al., 1998). MdmX did not possess those motifs, thereby, mainly localizing within the cytoplasm (Li et al., 2002). However, dimerization with Mdm2 via their C-terminal RING domains could allow transport of MdmX into the nucleus. Nuclear localization of the Mdm2 RING and MdmX RING domains could be explained by a complex formation between the exogenous RING domains and the endogenous Mdm2 that could transport them into the nucleus. Uniform localization of the Mdm2 and MdmX RING domains suggested their ability to regulate Mdm2 and MdmX functions within the nucleus and the cytoplasm.

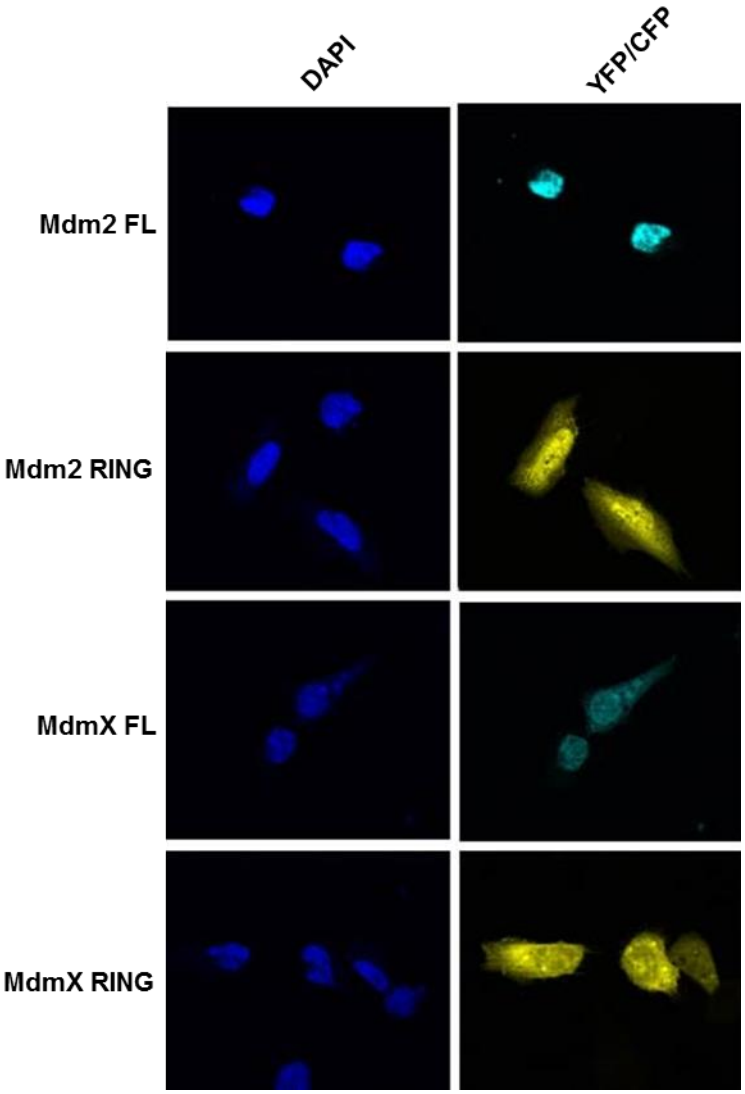

Figure 23. Cellular localization of the ectopically expressed Mdm2 RING and MdmX RING domains. Wild-type full-length Mdm2 and MdmX were expressed as CFP-fusion proteins; Mdm2 and MdmX RING were expressed as YFP-fusion proteins. U2OS cells were transfected with CFP-Mdm2, CFP-MdmX, YFP-Mdm2 RING, and YFP-MdmX RING. Cells were fixed at 24 hours post-transfection. Nuclei were stained with DAPI. Results indicate nuclear localization of the full-length Mdm2 and overlapping nuclear and cytoplasmic localization of the full-length MdmX, Mdm2 RING, and MdmX RING domains.

3.3.7. Interaction of the full-length Mdm2 and MdmX with the Mdm2 RING and MdmX RING domains in vivo

To analyze interactions of the full-length Mdm2 and MdmX with the Mdm2 RING and MdmX RING domains *in vivo*, co-immunoprecipitation experiments were conducted using the U2OS cell line (Figures 24 and 25). U2OS cells were co-transfected with either CFP-Mdm2 FL or CFP-MdmX FL and either FLAG-Mdm2 RING or FLAG-MdmX RING. Empty FLAG vector was also transfected with either CFP-Mdm2 FL or CFP-MdmX RING and was used as a negative control. FLAG-Mdm2 RING or FLAG-MdmX RING was pulled down from the cell lysates with a polyclonal anti-FLAG antibody. Immunoblotting was used to analyze the presence of protein-protein interactions. FLAG-tagged RING domains were detected with a monoclonal anti-FLAG antibody. Mdm2 FL and MdmX FL proteins that could co-immunoprecipitate with the FLAG-RING domains in case of complex formation were identified with monoclonal anti-Mdm2 or anti-MdmX antibodies. As a result of co-immunoprecipitation experiments, Mdm2 FL was found to interact with both FLAG-Mdm2 RING and FLAG-MdmX RING domains (Figure 24A and 24B). Complex formation between MdmX FL and FLAG-Mdm2 RING or FLAG-MdmX RING was also observed (Figure 25A and 25B). These experiments supported the notion that Mdm2 FL and MdmX FL could form dimers with Mdm2 RING and MdmX RING via their C-terminal RING domains.

A.

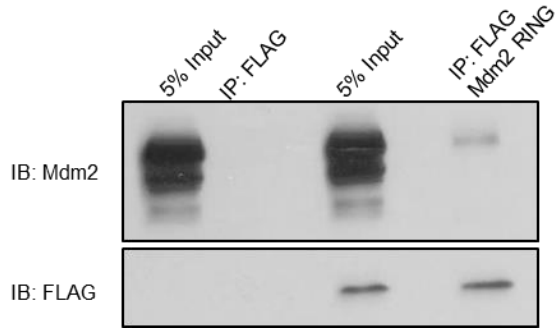

B.

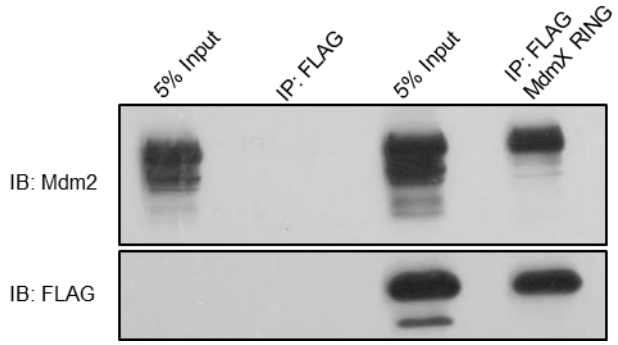

Figure 24. Mdm2 interacts with Mdm2 RING and MdmX RING *in vivo*. U2OS cells were co-transfected with an empty FLAG vector and CFP-Mdm2 FL to serve as a negative control; FLAG-Mdm2 RING or FLAG-MdmX RING and CFP-Mdm2 FL to test the interaction. Co-immunoprecipitation was carried out 24 hours post-transfection using a polyclonal anti-FLAG antibody. *A* and *B,* Immunoblotting was carried out with monoclonal anti-Mdm2 (1:1000) and monoclonal anti-FLAG (1:1000) antibodies.

A.

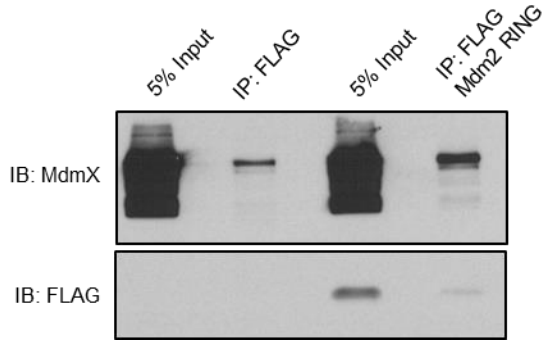

B.

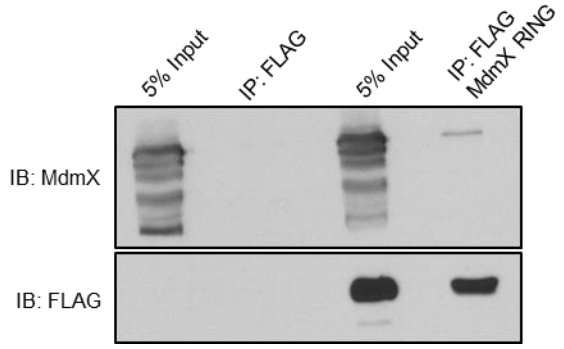

Figure 25. MdmX interacts with Mdm2 RING and MdmX RING *in vivo*. U2OS cells were co-transfected with an empty FLAG vector and CFP-MdmX FL to serve as a negative control; FLAG-Mdm2 RING or FLAG-MdmX RING and CFP-MdmX FL to test the interaction. Co-immunoprecipitation was carried out 24 hours post-transfection using a polyclonal anti-FLAG antibody. *A* and *B*, Immunoblotting was carried out with anti-MdmX (1:1000) and anti-Flag (1:1000) antibodies.

3.4. Discussion

The purpose of this study was to carry out a functional analysis of the Mdm2 and MdmX RING domains *in vivo*. An approach of ectopic expression of the RING domains in a human osteosarcoma U2OS cell line was taken. Following a 24-hour transfection period, we observed the effects of the exogenous proteins on the levels of endogenous p53 and its main negative regulators Mdm2 and MdmX. Furthermore, gene transcription activity of p53 by means of detecting levels of phosphorylated p53 and its downstream gene targets, namely p21 and Bax was examined. The effects of the exogenous proteins were compared between normal and stress conditions, triggered by the DNA-damaging agent doxorubicin. Localization of the overexpressed Mdm2 FL, MdmX FL, Mdm2 RING and MdmX RING domains in U2OS cells was detected. Lastly, interactions of the wild-type full-length Mdm2 and MdmX with the Mdm2 RING and MdmX RING domains were shown *in vivo*.

Following ectopic expression of Mdm2 FL under normal or stress conditions, an increased cellular Mdm2 level and decreased endogenous p53, phosphorylated p53, and p21 levels were found. There were no changes in the endogenous levels of MdmX and Bax. Low p53 levels could be explained by the Mdm2-mediated p53 polyubiquitination, which targeted it for the proteasomal degradation. Consequently, low levels of the phosphorylated p53 and p21 were observed. This was further supported by the fact that Mdm2 FL was primarily localized within the nucleus. In addition, several studies showed Mdm2-dependent destabilization of p21, which could also contribute to the observed low p21 level (Zhang et al., 2004; Jin et al., 2003).

Overexpression of MdmX FL did not affect levels of the endogenous Mdm2 and Bax regardless of doxorubicin administration. Interestingly, under normal conditions we observed a slight accumulation of p53 and phosphorylated p53, and low levels of p21 expression. Following doxorubicin treatment these effects were not found. Different cell responses to MdmX overexpression indicated functional complexity and differential recruitment of MdmX in normal and stress conditions. An increase in the levels of p53 and phosphorylated p53 could occur as a result of inhibition of the Mdm2-mediated p53 degradation by means of complex formation between Mdm2 and MdmX. Although, p53 was stabilized in the cell, it was transcriptionally inactive as exemplified by the levels of p21. This effect was probably seen due to the MdmX-dependent inhibition of the p53 gene transcription activity through interactions between their N-terminal domains. This explanation seems plausible since MdmX FL was found partially localized within the nucleus while predominantly appearing in the cytoplasm. In addition, low p21 level in a sample with the overexpressed MdmX FL could also be explained by several studies that demonstrated MdmX-mediated p21 degradation independent of p53 (Lee and Lu, 2011; Jin et al., 2008). It is important to mention that in contrast to several studies, we did not find Mdm2 stabilization by MdmX and efficient p53 degradation by the Mdm2/MdmX heterodimer (Sharp et al., 1999; Stad et al., 2001). The underlying mechanism for this contradiction is not clear; however, it should be addressed in later experiments.

In absence of doxorubicin treatment, ectopically expressed Mdm2 RING domain led to a slight stabilization of the endogenous Mdm2 and no changes in MdmX, p53, phosphorylated p53, p21 and Bax levels. Following drug treatment, more efficient

stabilization of the endogenous Mdm2, an increase in phosphorylated p53 level, and p21 expression were observed. No significant changes in MdmX, p53, and Bax levels were found in presence of a stress signal. Co-immunoprecipitation experiments demonstrated the ability of the overexpressed Mdm2 RING to interact with full-length Mdm2 and MdmX *in vivo*. Dimerization with Mdm2 could explain nuclear translocalization of the exogenous Mdm2 RING from the cytoplasm. Therefore, the observed Mdm2 stabilization in stress conditions could be explained by the dimer formation between the endogenous Mdm2 and exogenous Mdm2 RING domain, which led to inhibition of Mdm2 autoubiquitination activity and its degradation. The endogenous MdmX level did not seem to be affected since MdmX did not possess intrinsic ubiquitination activity. Observed increased levels of p21 under stress conditions indicated that Mdm2 RING inhibited interactions between Mdm2 and p53 enabling p53 to perform transactivation activity. It could be concluded that Mdm2 RING acted in a dominant negative fashion to suppress Mdm2 E3 ligase function and specifically in presence of a DNA-damaging signal prevented Mdm2-mediated inhibition of the p53 gene transcription activity.

Under normal and stress conditions stabilization of the endogenous Mdm2 and MdmX as a result of MdmX RING overexpression was observed, while there was no effect on p53, phosphorylated p53, and Bax levels. A decrease and no change in p21 expression were found in absence and presence of a stress signal, respectively. The MdmX RING domain was shown to interact with full-length Mdm2 and MdmX *in vivo*. Similar to the exogenous Mdm2 RING, ectopically expressed MdmX RING domain was located in the nucleus and the cytoplasm. Nuclear localization of MdmX RING could be

attributed to the interaction with Mdm2. Stabilization of the endogenous Mdm2 and MdmX could be a consequence of inhibition of the Mdm2 E3 ligase activity by means of complex formation between the ectopically expressed MdmX RING and the endogenous Mdm2. A decrease and no change in p21 levels resulted from the Mdm2 and MdmX-dependent suppression of the p53 transcriptional activity through interactions between their N-terminal domains. These findings indicated that the exogenous MdmX RING domain, like Mdm2 RING, exhibited a dominant negative phenotype inhibiting Mdm2 ubiquitination activity leading to its stabilization, which in turn demonstrated a negative effect on p53 gene transcription activity.

Current findings imply that Mdm2 RING and MdmX RING function differently in cells depending on presence or absence of stress stimuli. Even though further investigation is necessary to understand the cause for no changes in a pro-apoptotic Bax expression, differences in p21 expression were observed. The comparison of the Mdm2 and MdmX RING domains made in this study, an observed inhibitory effect of the Mdm2 function represented advances towards a functional characterization of the RING domains *in vivo*, which is crucial for developing anti-cancer drug treatment.

CHAPTER 4: Concluding remarks

Regulation of p53 by its negative regulators Mdm2 and MdmX is crucial for proper cellular functioning and prevention of tumourigenesis. Mdm2-mediated ubiquitination of p53 remains the main mechanism maintaining its cellular stability.

A comparative study of the homologous Mdm2 and MdmX RING domains investigating specific residues within the E2 binding and dimerization regions important for the E3 ligase activity was performed in this study. It is crucial to gather understanding of the effects of the introduced mutations on the ubiquitin transfer mechanism on the atomic level through obtaining MdmX RING mutant homodimer and MdmX RING mutant-E2 complex structures. In this study, MdmX RING N448C/K478R mutant was shown to ubiquitinate wild-type full-length MdmX. It would be interesting to introduce those mutations into the full-length MdmX to test its ability to ubiquitinate p53 *in vitro*. Importantly, the effect of the amino acid substitutions within the MdmX RING domain that granted it E3 ligase activity *in vitro* should be tested *in vivo*. In particular, the ability of the activated MdmX RING domains to perform Mdm2 and p53 ubiquitination should be examined in cells.

Moreover, functional effects of the ectopic expression of the Mdm2 and MdmX RING domains in U2OS cells were analyzed. To further understand p53 gene transcription activity in presence of the ectopically expressed Mdm2 RING and MdmX RING domains, phosphorylation sites other than serine 15 and acetylation of the C-terminal lysine residues should be investigated. Functional assays aimed to analyze cell

proliferation and apoptosis of the cells with ectopically expressed Mdm2 RING and MdmX RING domains should be also carried out. Finally, ubiquitination of the endogenous Mdm2, MdmX, and p53 following ectopic expression of Mdm2 RING and MdmX RING domains should be examined. To carry out this analysis, cells should be treated with a proteasome inhibitor – MG132. Following drug treatment, ubiquitinated endogenous proteins can be detected in cell lysates via immunoblotting. These findings support necessity for the future characterization of the Mdm2 and MdmX RING domains *in vitro* and *in vivo* to further understand the mechanism of the Mdm2 RING E3 ligase activity.

Together, this study provides a structural and molecular insight into the composition of the active site of the Mdm2 RING domain responsible for the ubiquitin transfer and elucidates the effects of the oncogenic properties of the Mdm2 and MdmX RING domains *in vivo*.

REFERENCES

Allende-Vega, N., and Saville, M.K. (2010). Targeting the ubiquitin-proteasome system to activate wild-type p53 for cancer therapy. Semin. Cancer Biol. *20*, 29-39.

Brooks, C.L., Li, M., and Gu, W. (2004). Monoubiquitination: the signal for p53 nuclear export? Cell cycle *3*, 436-438.

Brooks, C.L., and Gu, W. (2010). New insights into p53 activation. Cell Res. *20*, 614-621.

Brooks, S.A. (2010). Functional interactions between mRNA turnover and surveillance and the ubiquitin proteasome system. Wiley Interdiscip. Rev. RNA *1*, 240-252.

Bottger, V., Bottger, A., Garcia-Echeverria, C., Ramos, Y.F., van der Eb, A.J., Jochemsen, A.G., and Lane, D.P. (1999). Comparative study of the p53-mdm2 and p53-MDMX interfaces. Oncogene *18*, 189-199.

Chang, C., Simmons, D.T., Martin, M.A., and Mora, P.T. (1979). Identification and partial characterization of new antigens from simian virus 40-transformed mouse cells. J. Virol. *31*, 463-471.

Chang, J., Kim, D.H., Lee, S.W., Choi, K.Y., and Sung, Y.C. (1995). Transactivation ability of p53 transcriptional activation domain is directly related to the binding affinity to TATA-binding protein. J. Biol. Chem. *270*, 25014-25019.

Chen, J., Lin, J., and Levine, A.J. (1995). Regulation of transcription functions of the p53 tumor suppressor by the mdm-2 oncogene. Mol. Med. *1*, 142-152.

Chen, L., Agrawal, S., Zhou, W., Zhang, R., and Chen, J. (1998). Synergistic activation of p53 by inhibition of MDM2 expression and DNA damage. Proc. Natl. Acad. Sci. U S A *95*, 195-200.

Dang, J., Kuo, M.L., Eischen, C.M., Stepanova, L., Sherr, C.J., and Roussel, M.F. (2002). The RING domain of Mdm2 can inhibit cell proliferation. Cancer Res. *62*, 1222-1230.

Davydov, I.V., Woods, D., Safiran, Y.J., Oberoi, P., Fearnhead, H.O., Fang, S., Jensen, J.P., Weissman, A.M., Kenten, J.H., and Vousden, K.H. (2004). Assay for ubiquitin ligase activity: high-throughput screen for inhibitors of HDM2. J. Biomol. Screen. *9*, 695-703.

DeLeo, A.B., Jay, G., Appella, E., Dubois, G.C., Law, L.W., and Old, L.J. (1979). Detection of a transformation-related antigen in chemically induced sarcomas and other transformed cells of the mouse. Proc. Natl. Acad. Sci. U S A *76*, 2420-2424.

Dickens, M.P., Fitzgerald, R., and Fischer, P.M. (2010). Small-molecule inhibitors of MDM2 as new anticancer therapeutics. Semin. Cancer Biol. *20*, 10-18.

Dikic, I., Wakatsuki, S., and Walters, K.J. (2009). Ubiquitin-binding domains - from structures to functions. Nat. Rev. Mol. Cell. Biol. *10*, 659-671.

Ding, K., Lu, Y., Nikolovska-Coleska, Z., Wang, G., Qiu, S., Shangary, S., Gao, W., Qin, D., Stuckey, J., Krajewski, K., *et al.* (2006). Structure-based design of spiro-oxindoles as potent, specific small-molecule inhibitors of the MDM2-p53 interaction. J. Med. Chem. *49*, 3432-3435.

Dumaz, N., and Meek, D.W. (1999). Serine15 phosphorylation stimulates p53 transactivation but does not directly influence interaction with HDM2. EMBO J. *18*, 7002-7010.

el-Deiry, W.S., Tokino, T., Velculescu, V.E., Levy, D.B., Parsons, R., Trent, J.M., Lin, D., Mercer, W.E., Kinzler, K.W., and Vogelstein, B. (1993). WAF1, a potential mediator of p53 tumor suppression. Cell *75*, 817-825.

el-Deiry, W.S., Harper, J.W., O'Connor, P.M., Velculescu, V.E., Canman, C.E., Jackman, J., Pietenpol, J.A., Burrell, M., Hill, D.E., Wang, Y., *et al.* (1994). WAF1/CIP1 is induced in p53-mediated G1 arrest and apoptosis. Cancer Res. *54*, 1169-1174.

Evans, S.C., Viswanathan, M., Grier, J.D., Narayana, M., El-Naggar, A.K., and Lozano, G. (2001). An alternatively spliced HDM2 product increases p53 activity by inhibiting HDM2. Oncogene *20*, 4041-4049.

Fang, S., Jensen, J.P., Ludwig, R.L., Vousden, K.H., and Weissman, A.M. (2000). Mdm2 is a RING finger-dependent ubiquitin protein ligase for itself and p53. J. Biol. Chem. *275*, 8945-8951.

Fakharzadeh, S.S., Rosenblum-Vos, L., Murphy, M., Hoffman, E.K., and George, D.L. (1993). Structure and organization of amplified DNA on double minutes containing the mdm2 oncogene. Genomics *15*, 283-290.

Foord, O.S., Bhattacharya, P., Reich, Z., and Rotter, V. (1991). A DNA binding domain is contained in the C-terminus of wild type p53 protein. Nucleic Acids Res. *19*, 5191-5198.

Freemont, P.S. (1993). The RING finger. A novel protein sequence motif related to the zinc finger. Ann. N. Y. Acad. Sci. *684*, 174-192.

Fridman, J.S., Hernando, E., Hemann, M.T., de Stanchina, E., Cordon-Cardo, C., and Lowe, S.W. (2003). Tumor promotion by Mdm2 splice variants unable to bind p53. Cancer Res. *63*, 5703-5706.

Friedman, P.N., Chen, X., Bargonetti, J., and Prives, C. (1993). The p53 protein is an unusually shaped tetramer that binds directly to DNA. Proc. Natl. Acad. Sci. U S A *90*, 3319-3323.

Geyer, R.K., Yu, Z.K., and Maki, C.G. (2000). The MDM2 RING-finger domain is required to promote p53 nuclear export. Nat. Cell Biol. *2*, 569-573.

Giglio, S., Mancini, F., Gentiletti, F., Sparaco, G., Felicioni, L., Barassi, F., Martella, C., Prodosmo, A., Iacovelli, S., Buttitta, F., *et al.* (2005). Identification of an aberrantly spliced form of HDMX in human tumors: a new mechanism for HDM2 stabilization. Cancer Res. *65*, 9687-9694.

Groettrup, M., Pelzer, C., Schmidtke, G., and Hofmann, K. (2008). Activating the ubiquitin family: UBA6 challenges the field. Trends Biochem. Sci. *33*, 230-237.

Gu, W., and Roeder, R.G. (1997). Activation of p53 sequence-specific DNA binding by acetylation of the p53 C-terminal domain. Cell *90*, 595-606.

Gu, J., Nie, L., Wiederschain, D., and Yuan, Z.M. (2001). Identification of p53 sequence elements that are required for MDM2-mediated nuclear export. Mol. Cell. Biol. *21*, 8533-8546.

Gu, B., and Zhu, W.G. (2012). Surf the post-translational modification network of p53 regulation. Int. J. Biol. Sci. *8*, 672-684.

Hammond-Martel, I., Yu, H., and Affar el, B. (2012). Roles of ubiquitin signaling in transcription regulation. Cell. Signal. *24*, 410-421.

Haupt, Y., Maya, R., Kazaz, A., and Oren, M. (1997). Mdm2 promotes the rapid degradation of p53. Nature *387*, 296-299.

Haupt, S., Berger, M., Goldberg, Z., and Haupt, Y. (2003). Apoptosis - the p53 network. J. Cell Sci. *116*, 4077-4085.

Hershko, A., and Ciechanover, A. (1998). The ubiquitin system. Annu. Rev. Biochem. *67*, 425-479.

Honda, R., Tanaka, H., and Yasuda, H. (1997). Oncoprotein MDM2 is a ubiquitin ligase E3 for tumor suppressor p53. FEBS Lett. *420*, 25-27.

Issaeva, N., Bozko, P., Enge, M., Protopopova, M., Verhoef, L.G., Masucci, M., Pramanik, A., and Selivanova, G. (2004). Small molecule RITA binds to p53, blocks p53-HDM-2 interaction and activates p53 function in tumors. Nat. Med. *10*, 1321-1328.

Iwakuma, T., and Lozano, G. (2003). MDM2, an introduction. Mol. Cancer Res. *1*, 993-1000.

Iyappan, S., Wollscheid, H.P., Rojas-Fernandez, A., Marquardt, A., Tang, H.C., Singh, R.K., and Scheffner, M. (2010). Turning the RING domain protein MdmX into an active ubiquitin-protein ligase. J. Biol. Chem. *285*, 33065-33072.

Jamal, S., and Ziff, E.B. (1995). Raf phosphorylates p53 in vitro and potentiates p53-dependent transcriptional transactivation in vivo. Oncogene *10*, 2095-2101.

Jin, Y., Lee, H., Zeng, S. X., Dai, M.-S., and Lu, H. (2003). MDM2 promotes $p21^{waf1/cip1}$ proteasomal turnover independently of ubiquitylation. EMBO J. *22*, 6365-6377.

Jin, Y., Zeng, S.X., Sun, X.X., Lee, H., Blattner, C., Xiao, Z., and Lu, H. (2008). MDMX promotes proteasomal turnover of p21 at G1 and early S phases independently of, but in cooperation with, MDM2. Mol. Cell. Biol. *28*, 1218-1229.

Jones, S.N., Roe, A.E., Donehower, L.A., and Bradley, A. (1995). Rescue of embryonic lethality in Mdm2-deficient mice by absence of p53. Nature *378*, 206-208.

Kawai, H., Wiederschain, D., and Yuan, Z.M. (2003). Critical contribution of the MDM2 acidic domain to p53 ubiquitination. Mol. Cell. Biol. *23*, 4939-4947.

Kessler, B.M. (2013). Ubiquitin - omics reveals novel networks and associations with human disease. Curr. Opin. Chem. Biol. *17*, 59-65.

Kimura, Y., and Tanaka, K. (2010). Regulatory mechanisms involved in the control of ubiquitin homeostasis. J. Biochem. *147*, 793-798.

Kitagaki, J., Agama, K.K., Pommier, Y., Yang, Y., and Weissman, A.M. (2008). Targeting tumor cells expressing p53 with a water-soluble inhibitor of Hdm2. Mol. Cancer Ther. *7*, 2445-2454.

Kostic, M., Matt, T., Martinez-Yamout, M.A., Dyson, H.J., and Wright, P.E. (2006). Solution structure of the Hdm2 C2H2C4 RING, a domain critical for ubiquitination of p53. J. Mol. Biol. *363*, 433-450.

Kubbutat, M.H., Jones, S.N., and Vousden, K.H. (1997). Regulation of p53 stability by Mdm2. Nature *387*, 299-303.

Lai, Z., Yang, T., Kim, Y.B., Sielecki, T.M., Diamond, M.A., Strack, P., Rolfe, M., Caligiuri, M., Benfield, P.A., Auger, K.R., *et al.* (2002). Differentiation of Hdm2-mediated p53 ubiquitination and Hdm2 autoubiquitination activity by small molecular weight inhibitors. Proc. Natl. Acad. Sci. U S A *99*, 14734-14739.

Lane, D.P., and Crawford, L.V. (1979). T antigen is bound to a host protein in SV40-transformed cells. Nature *278*, 261-263.

Lane, D.P. (1992). Cancer. p53, guardian of the genome. Nature *358*, 15-16.

Lee, J.T., and Gu, W. (2010). The multiple levels of regulation by p53 ubiquitination. Cell Death Differ. *17*, 86-92.

Lee, J.-H., and Lu, H. (2011). 14-3-3γ Inhibition of MDMX-mediated p21 turnover independent of p53. J. Biol. Chem. *286*, 5136-5142.

Lenos, K., and Jochemsen, A.G. (2011). Functions of MDMX in the modulation of the p53-response. J. Biomed. Biotechnol. *2011*, 876173.

Lenos, K., Grawenda, A.M., Lodder, K., Kuijjer, M.L., Teunisse, A.F., Repapi, E., Grochola, L.F., Bartel, F., Hogendoorn, P.C., Wuerl, P., *et al.* (2012). Alternate splicing of the p53 inhibitor HDMX offers a superior prognostic biomarker than p53 mutation in human cancer. Cancer Res. *72*, 4074-4084.

Levine, A.J. (1997). p53, the cellular gatekeeper for growth and division. Cell *88*, 323-331.

Li, C., Chen, L., and Chen, J. (2002). DNA damage induces MDMX nuclear translocation by p53-dependent and -independent mechanisms. Mol. Cell. Biol. *22*, 7562-7571.

Lindstrom, M.S., Jin, A., Deisenroth, C., White Wolf, G., and Zhang, Y. (2007). Cancer-associated mutations in the MDM2 zinc finger domain disrupt ribosomal protein interaction and attenuate MDM2-induced p53 degradation. Mol. Cell. Biol. *27*, 1056-1068.

Linke, K., Mace, P.D., Smith, C.A., Vaux, D.L., Silke, J., and Day, C.L. (2008). Structure of the MDM2/MDMX RING domain heterodimer reveals dimerization is required for their ubiquitylation in trans. Cell Death Differ. *15*, 841-848.

Linzer, D.I., and Levine, A.J. (1979). Characterization of a 54K dalton cellular SV40 tumor antigen present in SV40-transformed cells and uninfected embryonal carcinoma cells. Cell *17*, 43-52.

Lohrum, M.A., Ashcroft, M., Kubbutat, M.H., and Vousden, K.H. (2000). Identification of a cryptic nucleolar-localization signal in MDM2. Nat. Cell. Biol. *2*, 179-181.

Loughery, J., and Meek, D. (2013). Switching on p53: an essential role for protein phosphorylation? Biodiversity *8*, DOI:10.7750.

Mace, P.D., Linke, K., Feltham, R., Schumacher, F.R., Smith, C.A., Vaux, D.L., Silke, J., and Day, C.L. (2008). Structures of the cIAP2 RING domain reveal conformational changes associated with ubiquitin-conjugating enzyme (E2) recruitment. J. Biol. Chem. *283*, 31633-31640.

Malkin, D., Li, F.P., Strong, L.C., Fraumeni, J.F., Jr., Nelson, C.E., Kim, D.H., Kassel, J., Gryka, M.A., Bischoff, F.Z., Tainsky, M.A., *et al.* (1990). Germ line p53 mutations in a familial syndrome of breast cancer, sarcomas, and other neoplasms. Science *250*, 1233-1238.

Marchenko, N.D., Wolff, S., Erster, S., Becker, K., and Moll, U.M. (2007). Monoubiquitylation promotes mitochondrial p53 translocation. EMBO J. *26*, 923-934.

Meek, D.W., and Anderson, C.W. (2009). Posttranslational modification of p53: cooperative integrators of function. Cold Spring Harb. Perspect. Biol. *1*, a000950.

Melero, J.A., Stitt, D.T., Mangel, W.F., and Carroll, R.B. (1979). Identification of new polypeptide species (48-55K) immunoprecipitable by antiserum to purified large T antigen and present in SV40-infected and -transformed cells. Virology *93*, 466-480.

Metzger, M.B., Hristova, V.A., and Weissman, A.M. (2012). HECT and RING finger families of E3 ubiquitin ligases at a glance. J. Cell Sci. *125*, 531-537.

Momand, J., Zambetti, G.P., Olson, D.C., George, D., and Levine, A.J. (1992). The mdm-2 oncogene product forms a complex with the p53 protein and inhibits p53-mediated transactivation. Cell *69*, 1237-1245.

Momand, J., Jung, D., Wilczynski, S., and Niland, J. (1998). The MDM2 gene amplification database. Nucleic Acids Res. *26*, 3453-3459.

Montes de Oca Luna, R., Wagner, D. S., Lozano, G. (1995). Rescue of early embryonic lethality in mdm2-deficient mice by deletion of p53. Nature *378*, 203-206.

Oliner, J.D., Kinzler, K.W., Meltzer, P.S., George, D.L., and Vogelstein, B. (1992). Amplification of a gene encoding a p53-associated protein in human sarcomas. Nature *358*, 80-83.

Pan, Y., and Chen, J. (2003). MDM2 promotes ubiquitination and degradation of MDMX. Mol. Cell. Biol. *23*, 5113-5121.

Parant, J., Chavez-Reyes, A., Little, N.A., Yan, W., Reinke, V., Jochemsen, A.G., and Lozano, G. (2001). Rescue of embryonic lethality in Mdm4-null mice by loss of Trp53 suggests a nonoverlapping pathway with MDM2 to regulate p53. Nat. Genet. *29*, 92-95.

Perry, M.E. (2010). The regulation of the p53-mediated stress response by MDM2 and MDM4. Cold Spring Harb. Perspect. Biol. *2*, a000968.

Poyurovsky, M.V., Jacq, X., Ma, C., Karni-Schmidt, O., Parker, P.J., Chalfie, M., Manley, J.L., and Prives, C. (2003). Nucleotide binding by the Mdm2 RING domain facilitates Arf-independent Mdm2 nucleolar localization. Mol. Cell *12*, 875-887.

Poyurovsky, M.V., Priest, C., Kentsis, A., Borden, K.L., Pan, Z.Q., Pavletich, N., and Prives, C. (2007). The Mdm2 RING domain C-terminus is required for supramolecular assembly and ubiquitin ligase activity. EMBO J. *26*, 90-101.

Priest, C., Prives, C., and Poyurovsky, M.V. (2010). Deconstructing nucleotide binding activity of the Mdm2 RING domain. Nucleic Acids Res. *38*, 7587-7598.

Rivlin, N., Brosh, R., Oren, M., and Rotter, V. (2011). Mutations in the p53 Tumor Suppressor Gene: Important Milestones at the Various Steps of Tumorigenesis. Genes Cancer *2*, 466-474.

Roth, J., Dobbelstein, M., Freedman, D.A., Shenk, T., and Levine, A.J. (1998). Nucleo-cytoplasmic shuttling of the hdm2 oncoprotein regulates the levels of the p53 protein via a pathway used by the human immunodeficiency virus rev protein. EMBO J. *17*, 554-564.

Sasiela, C.A., Stewart, D.H., Kitagaki, J., Safiran, Y.J., Yang, Y., Weissman, A.M., Oberoi, P., Davydov, I.V., Goncharova, E., Beutler, J.A., *et al.* (2008). Identification of inhibitors for MDM2 ubiquitin ligase activity from natural product extracts by a novel high-throughput electrochemiluminescent screen. J. Biomol. Screen. *13*, 229-237.

Selvakumaran, M., Lin, H.K., Miyashita, T., Wang, H.G., Krajewski, S., Reed, J.C., Hoffman, B., and Liebermann, D. (1994). Immediate early up-regulation of bax expression by p53 but not TGF beta 1: a paradigm for distinct apoptotic pathways. Oncogene *9*, 1791-1798.

Shangary, S., Qin, D., McEachern, D., Liu, M., Miller, R.S., Qiu, S., Nikolovska-Coleska, Z., Ding, K., Wang, G., Chen, J., *et al.* (2008). Temporal activation of p53 by a specific MDM2 inhibitor is selectively toxic to tumors and leads to complete tumor growth inhibition. Proc. Natl. Acad. Sci. U S A *105*, 3933-3938.

Sharp, D.A., Kratowicz, S.A., Sank, M.J., and George, D.L. (1999). Stabilization of the MDM2 oncoprotein by interaction with the structurally related MDMX protein. J. Biol. Chem. *274*, 38189-38196.

Shloush, J., Vlassov, J.E., Engson, I., Duan, S., Saridakis, V., Dhe-Paganon, S., Raught, B., Sheng, Y., and Arrowsmith, C.H. (2011). Structural and functional comparison of the RING domains of two p53 E3 ligases, Mdm2 and Pirh2. J. Biol. Chem. *286*, 4796-4808.

Shvarts, A., Steegenga, W.T., Riteco, N., van Laar, T., Dekker, P., Bazuine, M., van Ham, R.C., van der Houven van Oordt, W., Hateboer, G., van der Eb, A.J., *et al.* (1996). MDMX: a novel p53-binding protein with some functional properties of MDM2. EMBO J. *15*, 5349-5357.

Shvarts, A., Bazuine, M., Dekker, P., Ramos, Y.F., Steegenga, W.T., Merckx, G., van Ham, R.C., van der Houven van Oordt, W., van der Eb, A.J., and Jochemsen, A.G. (1997). Isolation and identification of the human homolog of a new p53-binding protein, Mdmx. Genomics *43*, 34-42.

Stad, R., Little, N.A., Xirodimas, D.P., Frenk, R., van der Eb, A.J., Lane, D.P., Saville, M.K., and Jochemsen, A.G. (2001). Mdmx stabilizes p53 and Mdm2 via two distinct mechanisms. EMBO Rep. *2*, 1029-1034.

Stommel, J.M., Marchenko, N.D., Jimenez, G.S., Moll, U.M., Hope, T.J., and Wahl, G.M. (1999). A leucine-rich nuclear export signal in the p53 tetramerization domain: regulation of subcellular localization and p53 activity by NES masking. EMBO J. *18*, 1660-1672.

Tabernero, J., Dirix, L., Schoffski, P., Cervantes, A., Lopez-Martin, J.A., Capdevila, J., van Beijsterveldt, L., Platero, S., Hall, B., Yuan, Z., *et al.* (2011). A phase I first-in-human pharmacokinetic and pharmacodynamic study of serdemetan in patients with advanced solid tumors. Clin. Cancer Res. *17*, 6313-6321.

Tang, Y., Zhao, W., Chen, Y., Zhao, Y., and Gu, W. (2008). Acetylation is indispensable for p53 activation. Cell *133*, 612-626.

Tanimura, S., Ohtsuka, S., Mitsui, K., Shirouzu, K., Yoshimura, A., and Ohtsubo, M. (1999). MDM2 interacts with MDMX through their RING finger domains. FEBS Lett. *447*, 5-9.

Tao, W., and Levine, A.J. (1999). Nucleocytoplasmic shuttling of oncoprotein Hdm2 is required for Hdm2-mediated degradation of p53. Proc. Natl. Acad. Sci. U S A *96*, 3077-3080.

Thrower, J.S., Hoffman, L., Rechsteiner, M., and Pickart, C.M. (2000). Recognition of the polyubiquitin proteolytic signal. EMBO J. *19*, 94-102.

Tortora, G., Caputo, R., Damiano, V., Bianco, R., Chen, J., Agrawal, S., Bianco, A.R., and Ciardiello, F. (2000). A novel MDM2 anti-sense oligonucleotide has anti-tumor activity and potentiates cytotoxic drugs acting by different mechanisms in human colon cancer. Int. J. Cancer *88*, 804-809.

Vassilev, L.T., Vu, B.T., Graves, B., Carvajal, D., Podlaski, F., Filipovic, Z., Kong, N., Kammlott, U., Lukacs, C., Klein, C., *et al.* (2004). In vivo activation of the p53 pathway by small-molecule antagonists of MDM2. Science *303*, 844-848.

Venot, C., Maratrat, M., Dureuil, C., Conseiller, E., Bracco, L., and Debussche, L. (1998). The requirement for the p53 proline-rich functional domain for mediation of apoptosis is correlated with specific PIG3 gene transactivation and with transcriptional repression. EMBO J. *17*, 4668-4679.

Vogelstein, B., Lane, D., and Levine, A.J. (2000). Surfing the p53 network. Nature *408*, 307-310.

Volk, E.L., Fan, L., Schuster, K., Rehg, J.E., and Harris, L.C. (2009). The MDM2-a splice variant of MDM2 alters transformation in vitro and the tumor spectrum in both Arf- and p53-null models of tumorigenesis. Mol. Cancer Res. *7*, 863-869.

Wade, M., Wang, Y.V., and Wahl, G.M. (2010). The p53 orchestra: Mdm2 and Mdmx set the tone. Trends Cell Biol. *20*, 299-309.

Walker, K.K., and Levine, A.J. (1996). Identification of a novel p53 functional domain that is necessary for efficient growth suppression. Proc. Natl. Acad. Sci. U S A *93*, 15335-15340.

Wang, W., Ho, W.C., Dicker, D.T., MacKinnon, C., Winkler, J.D., Marmorstein, R., and El-Deiry, W.S. (2005). Acridine derivatives activate p53 and induce tumor cell death through Bax. Cancer Biol. Ther. *4*, 893-898.

Wu, X., Bayle, J.H., Olson, D., and Levine, A.J. (1993). The p53-mdm-2 autoregulatory feedback loop. Genes Dev. *7*, 1126-1132.

Yang, Y., Ludwig, R.L., Jensen, J.P., Pierre, S.A., Medaglia, M.V., Davydov, I.V., Safiran, Y.J., Oberoi, P., Kenten, J.H., Phillips, A.C., *et al.* (2005). Small molecule inhibitors of HDM2 ubiquitin ligase activity stabilize and activate p53 in cells. Cancer Cell *7*, 547-559.

Ye, Y., and Rape, M. (2009). Building ubiquitin chains: E2 enzymes at work. Nature reviews Mol. Cell Biol. *10*, 755-764.

Zhang, R., and Wang, H. (2003). Antisense oligonucleotide inhibitors of MDM2 oncogene expression. Methods Mol. Med. *85*, 205-222.

Zhang, Z., Wang, H., Li, M., Agrawa, S., Chen, X., and Zhang, R. (2004). MDM2 is a negative regulator of $p21^{WAF1/CIP1}$, independent of p53. J. Biol. Chem. *279*, 16000-16006.

APPENDIX A: Structural and computational modeling of the interaction between the small molecule inhibitors of Mdm2 and the Mdm2 RING domain

Introduction

Release of p53 from the Mdm2-mediated suppression in malignant cells is a desired strategy in anti-cancer therapy. One of the approaches to inhibit Mdm2 is to abolish its RING-mediated E3 ligase activity. Several classes of small-molecule inhibitors of the Mdm2 RING domain have already been identified by high-throughput screening methods. Bisarylurea was one of the first identified compounds that inhibited Mdm2-mediated p53 ubiquitination, but not autoubiquitination (Lai et al., 2002). Deazaflavin derivative HLI98 inhibited Mdm2-mediated p53 ubiquitination and autoubiquitination (Davydov et al., 2004). The disadvantage of HLI98 was low solubility and low potency (Davydov et al., 2004). Novel deazaflavin derivative HLI373 showed higher solubility and higher potency (Kitagaki et al., 2008). Acridine derivatives blocked p53 ubiquitination (Wang et al., 2005). Naturally occurring compound sempervirine was demonstrated to abolish p53 ubiquitination by Mdm2 and autoubiquitination (Sasiela et al., 2008). Compound 35, or JNJ-26854165, developed by Ortho Biotech and Johnson & Johnson led to activation and stabilization of p53 in cancer cells; however it did not interfere with the p53-Mdm2 ubiquitination (Tabernero et al., 2011). This compound is now in Phase-I clinical trials for treatment of solid tumours (Tabernero et al., 2011). Though these chemical compounds demonstrated the ability to suppress Mdm2-RING mediated E3 ligase activity, the mechanism of action remains unclear. Therefore,

characterization of the interactions between the Mdm2 RING domain and the inhibitors is essential for the rational drug design.

Materials and Methods

Protein preparation

The three-dimensional structure of the Mdm2/MdmX RING heterodimer was obtained from the Protein Data Bank for the molecular docking (PDB 2VJE). With the help of PocketPicker plugin and PyMol potential ligand binding sites were identified. Using AutoDockTools-1.5.4 software all water molecules were excluded from the file, and hydrogen atoms were added to all polar residues. The configured structure was saved in PDBQT file format.

Ligand preparation

The two-dimensional structures of the chemical compounds were obtained using eMolecules online service. They were converted to the three-dimensional structures with the help of OpenBabel software. They then were saved in PDBQT file format using AutoDockTools-1.5.4 software.

Molecular docking

The entire pocket within the Mdm2/MdmX RING heterodimer for docking of the chemical compounds was positioned within the Grid Box created using AutoDockTools-1.5.4 software. Docking analysis was performed with the help of Autodock Vina where

the pocket within selected Grid Box was kept constant. Protein:ligand complexes were viewed using PyMol software.

Results and Discussion

The crystal structure of the Mdm2/MdmX RING heterodimer was used to compute the putative binding pocket on the surface of the protein and analyze whether the small molecule inhibitors could fit in the binding pocket (Appendix A. Figure 1A). Chemical structures of the examined small molecule inhibitors are demonstrated in Appendix A Figure 1B. Three-dimensional models of the complexes between the Mdm2/MdmX RING heterodimer and deazaflavin 2 (HLI98C), deazaflavin derivative HLI373, acridine derivative, bisarylurea, sempervirine, and compound 35 (JNJ-26854165) were generated. The output represented the complex structure with the chemical compound being in its most favourable orientation. Moreover, quantification of the binding affinity of each compound under investigation was obtained and summarized in Appendix A Figure 2. The enlarged view of the pocket harbouring an inhibitor is depicted in Appendix A Figures 2A-2F. The three-dimensional models will be analyzed for the binding contacts between the Mdm2 RING domain and the compounds to propose the mechanism for the inhibition of the Mdm2-RING mediated E3 ligase activity.

A.

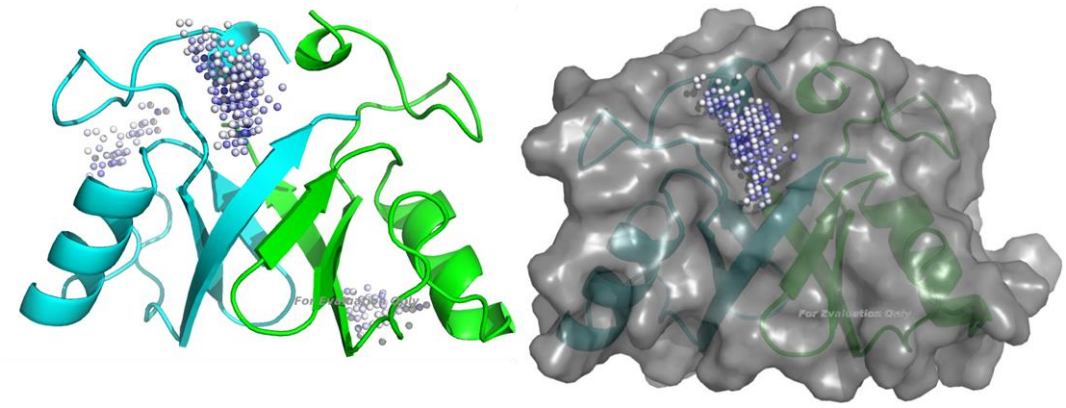

B.

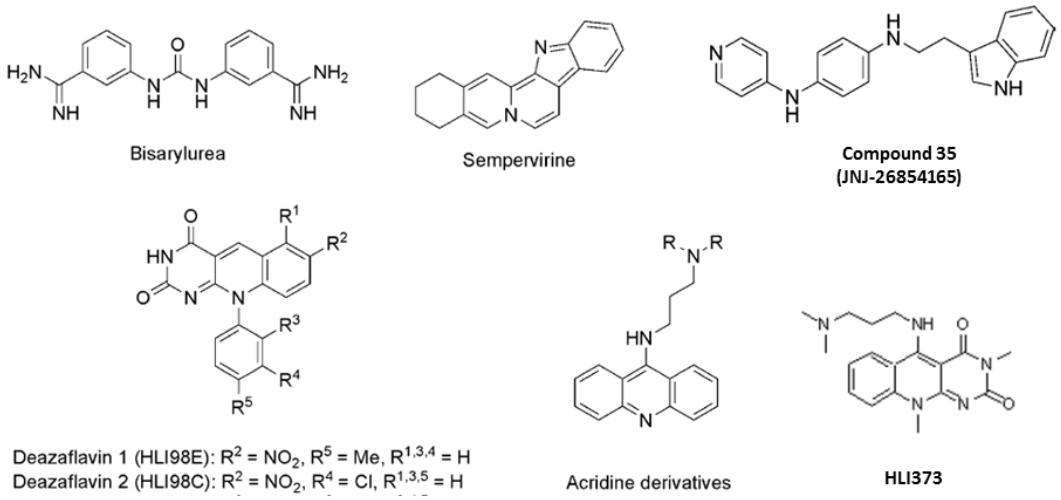

Appendix A. Figure 1. Structural analysis of the Mdm2/MdmX RING heterodimer. *A*, Cartoon model represents Mdm2/MdmX RING heterodimer (PDB 2VJE) with the potential pockets able to dock inhibitor compounds. *Left panel*, Mdm2 RING subunit is shown in green, MdmX RING – in cyan. Three binding pockets are shown with spheres. *Right panel*, Surface representation of the Mdm2/MdmX RING heterodimer (PDB 2VJE) with a pocket under investigation is depicted. *B*, Chemical formulas of the selected existing Mdm2 RING E3 ligase inhibitors are shown.

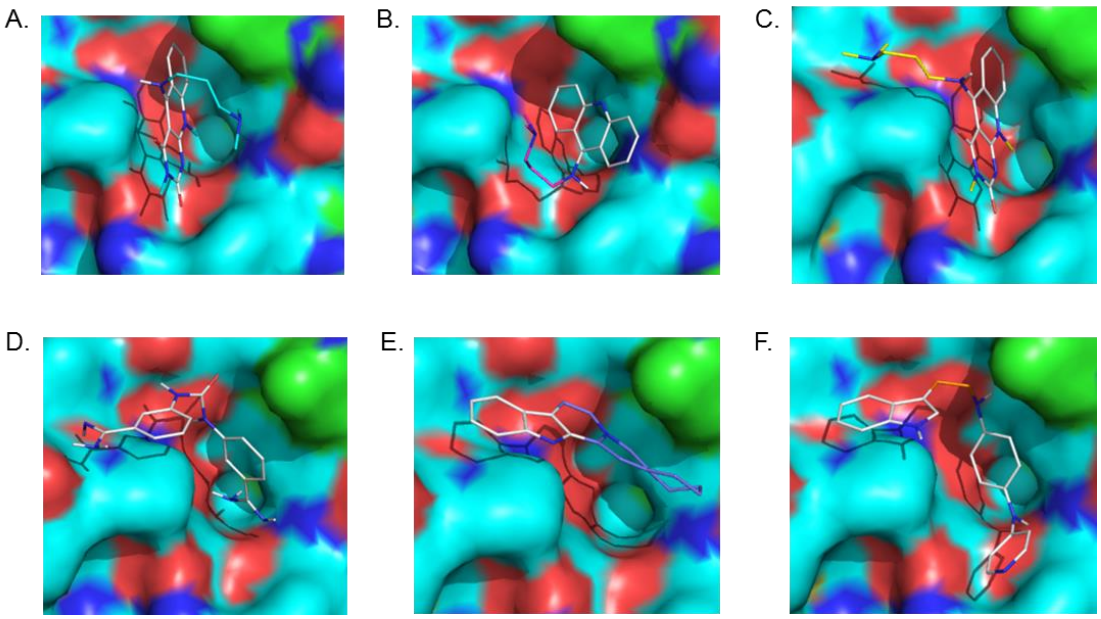

Ligands	Binding affinity (kcal/mol)
HLI 373	-5.0
Acridine derivative	-5.3
Deazaflavin 2 (HLI98C)	-6.1
Bisarylurea	-6.5
Sempervirine	-6.7
Compound 35	-7.0

Appendix A. Figure 2. Docking of the selected Mdm2 E3 ligase inhibitor compounds into the pocket under investigation. The enlarged views of the inhibitors docked into the pocket of the Mdm2/MdmX RING heterodimer (PDB 2VJE). Each compound in the complex is shown in its most favorable orientation. MGL tools AutoDock Vina software and PyMol were used to perform docking and generate computer models. *A*, HLI373; *B*, Acridine derivative; *C*, Deazaflavin 2 (HLI98C); *D*, Bisarylurea; *E*, Sempervirine; *F*, Compound 35 (JNJ-26854165). The binding affinities of these compounds are summarized in the table.

Future directions

Regardless of the existing data on the identified Mdm2 E3 ligase inhibitors, their effects should be verified with *in vitro* and *in vivo* ubiquitination assays. Particularly, experiments should be designed to test inhibition of the Mdm2 RING-mediated autoubiquitination or p53 ubiquitination. The binding affinities of the chemical compounds to Mdm2 RING should be further quantified using biophysical and biochemical methods such as Surface Plasmon Resonance.

Based on the results of the computational analysis, a number of the Mdm2 RING domain residues presumably involved in the interactions can be identified. The importance of these residues will be examined through site-directed mutagenesis followed by *in vitro* ubiquitination assays to test E3 ligase activity of the mutated Mdm2 RING domains. To further characterize the binding surface 2D-NMR experiments of the complexes between Mdm2 RING and inhibitors of interest should be performed. Finally, crystal trials for the Mdm2 RING:inhibitor complexes will be set up to obtain the atomic details of the interactions.

The data obtained from these experiments will be applied to improve design of the present or develop novel inhibitory compounds of the Mdm2 RING domain to achieve higher level of potency and specificity.

APPENDIX B: Supplementary figures

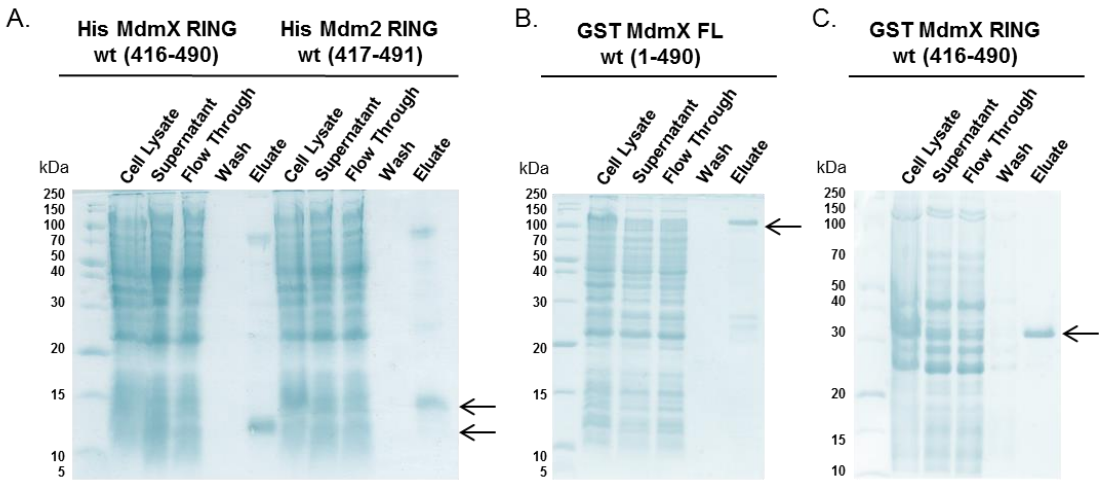

Appendix B. Figure 3. Purification of the wild-type proteins via affinity chromatography. *A,* His-tagged Mdm2 RING and MdmX RING domains were purified using nickel affinity chromatography. *B and C,* GST-fused MdmX FL and MdmX RING domain was purified using GST affinity chromatography. Purification samples were resolved on 15% SDS-PAGE and stained with Coomassie Brilliant Blue for visualization. Purification samples: cell lysate (sample of the bacterial cell lysate taken before sonication); supernatant (sample taken after sonication and centrifugation for isolation of the cell debris); flow through (sample taken after incubation with the resin); wash (sample taken following washing of the resin bound to the protein of interest); eluate (sample of the eluted protein).

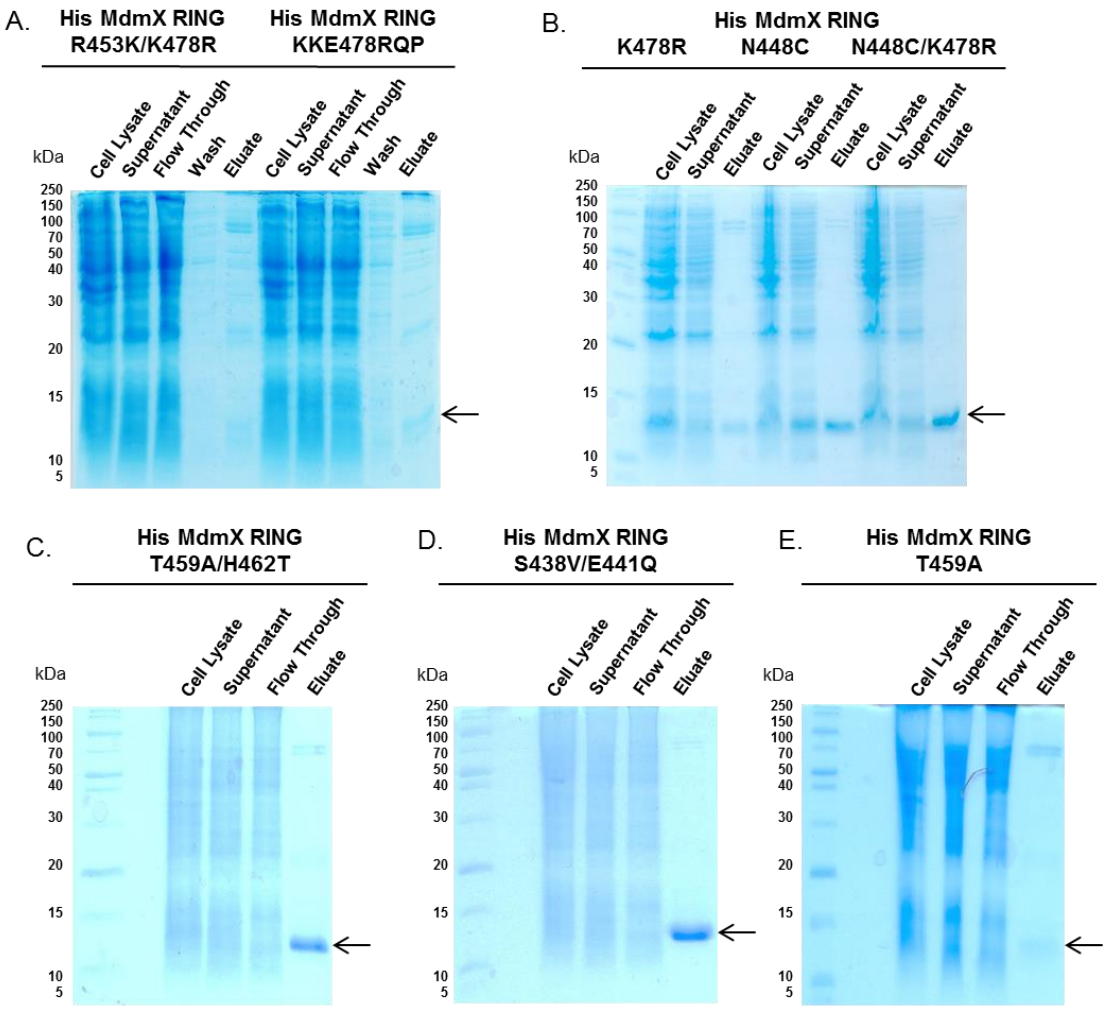

Appendix B. Figure 4. Purification of the mutated MdmX RING domains via affinity chromatography. His-tagged MdmX RING domain mutants were purified using nickel affinity chromatography. Purification samples were resolved on 15% SDS-PAGE and stained with Coomassie Brilliant Blue for visualization. Purification samples: cell lysate (sample of the bacterial cell lysate taken before sonication); supernatant (sample taken after sonication and centrifugation for isolation of the cell debris); flow through (sample taken after incubation with the resin); wash (sample taken following washing of the resin bound to the protein of interest); eluate (sample of the eluted protein).

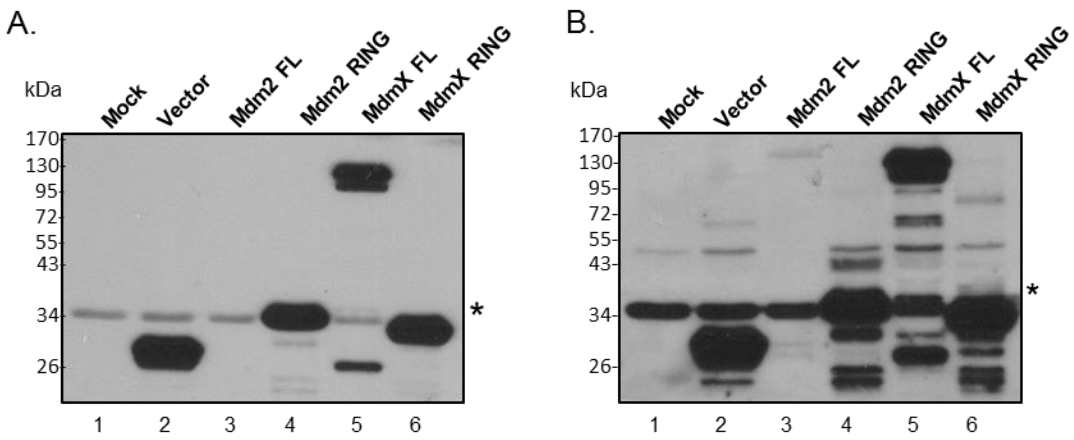

Appendix B. Figure 5. Expression level of the full-length CFP-Mdm2, CFP-MdmX, YFP-Mdm2 RING, and YFP-MdmX RING *in vivo*. Wild-type full-length Mdm2 and MdmX were expressed as CFP-fusion proteins; Mdm2 and MdmX RING were expressed as YFP-fusion proteins. U2OS cells were transfected with an empty YFP vector, CFP-Mdm2, CFP-MdmX, YFP-Mdm2 RING, and YFP-MdmX RING. *Mock* sample was prepared by treating cells with the transfection reagent alone with no DNA. Protein samples were prepared 24 hours post-transfection. Immunoblotting was carried out with a monoclonal anti-YFP antibody (1:1000). A monoclonal anti-GAPDH antibody was used to track GAPDH (indicated with a star (*)). *A*, 1 minute exposure. *B*, 30 minute exposure.

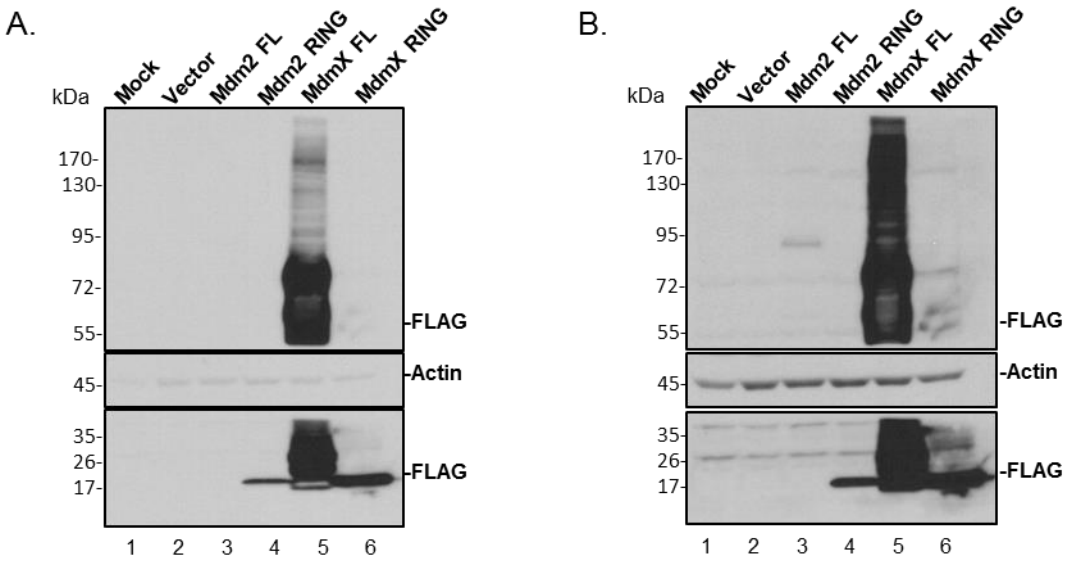

Appendix B. Figure 6. Expression level of the full-length FLAG-Mdm2, FLAG-MdmX, FLAG-Mdm2 RING, and FLAG-MdmX RING *in vivo*. Wild-type full-length Mdm2, MdmX, Mdm2 RING, and MdmX RING domains were expressed as FLAG-fusion proteins. U2OS cells were transfected with an empty FLAG vector, FLAG-Mdm2, FLAG-MdmX, FLAG-Mdm2 RING, and FLAG-MdmX RING. *Mock* sample was prepared by treating cells with the transfection reagent alone with no DNA. Protein samples were prepared 24 hours post-transfection and treated with 500 ng/ml of doxorubicin for 4 hours. Immunoblotting was carried out with a monoclonal anti-FLAG antibody (1:1000). A monoclonal anti-actin (1:1000) antibody was used to track actin. *A*, 1 minute exposure. *B*, 10 minute exposure.